Process design of a hydrogen production plant from natural gas with CO_2 capture based on a novel Ca/Cu chemical loop

I. Martínez [a,*], M.C. Romano [b], J.R. Fernández [c], P. Chiesa [b], R. Murillo [a], J.C. Abanades [c]

[a] Instituto de Carboquímica (Consejo Superior de Investigaciones Científicas), Miguel Luesma Castán 4, 50018 Zaragoza, Spain
[b] Politecnico di Milano, Dipartimento di Energia, Via Lambruschini 4, 20156 Milano, Italy
[c] Instituto Nacional del Carbón (Consejo Superior de Investigaciones Científicas), Francisco Pintado Fe 26, 33011 Oviedo, Spain

Received 25 May 2013
Received in revised form 13 September 2013
Accepted 15 September 2013

1. Background and scope

Hydrogen is mainly used today in ammonia, oil refining and methanol production plants. The share of hydrogen production in the global emissions of CO_2 is relatively small (the emissions from steam methane reformers are estimated to account for about 3% of the global emissions [1]), but the demand for hydrogen is expected to grow in the future due to the growth of ammonia production and to the increase in the use of H_2 for the production of light and low-sulphur oil distillates in hydrotreating and hydrocracking processes [2]. In addition, in a carbon-constrained world, the use of hydrogen as an energy carrier is expected to rise, in refineries as a fuel for power generation, in boilers and process heaters [3,4] or even as a fuel for transport assuming that the hydrogen economy continues to develop [5].

Synthesis gas (and therefore hydrogen) can be produced from almost any carbon source ranging from oil or natural gas to coal and biomass. Natural gas is the most widely used feedstock because of its low overall H_2 production costs at the most common

* Corresponding author. Tel.: +34 976 733977.
E-mail addresses: imartinez@icb.csic.es (I. Martínez), matteo.romano@polimi.it (M.C. Romano), jramon@incar.csic.es (J.R. Fernández), paolo.chiesa@polimi.it (P. Chiesa), ramon.murillo@csic.es (R. Murillo), abanades@incar.csic.es (J.C. Abanades).

Nomenclature

$e_{CO_2,NG}$	natural gas emission factor (2.65 kg CO_2/kg NG)
E_{eq}	equivalent CO_2 specific emission (g CO_2/MJ H_2 output)
$E_{eq\text{-}ref}$	equivalent CO_2 specific emission in the reference plant without capture (g CO_2/MJ H_2 output)
$\dot{m}_{CO_2,capt}$	mass flow rate of CO_2 captured
$\dot{m}_{H_2}$	mass flow rate of the H_2 output (kg/s)
$\dot{m}_{NG}$	mass flow rate of the natural gas input (kg/s)
$\dot{m}_{NG,eq}$	mass flow rate of the equivalent natural gas input (kg/s)
Q_{th}	thermal power output of the steam export (MW)
$T_{gin,i}$	gas temperature at the inlet of stage i of the Ca/Cu looping process (K)
$T_{max,i}$	maximum temperature achieved in stage i of the Ca/Cu looping process (K)
W_{el}	electricity power output of the plant (MW)

Acronyms

CCR	carbon capture ratio
CCR_{eq}	equivalent carbon capture ratio
CLC	chemical looping combustion
ECO	economiser
EVA	evaporator
FTR	fired tubular reformer
HP	high pressure
HT	high temperature
LHV	lower heating value
LT	low temperature
NG	natural gas
PSA	pressure swing adsorption
SER	sorption enhanced reforming
SH	superheater
SMR	steam methane reforming
SPECCA	specific primary energy consumption for CO_2 avoided
VLP	very low pressure
WGS	water gas shift

Greek letters

$\eta_{el,ref}$	electric efficiency of a conventional natural gas combined cycle
η_{eq,H_2}	equivalent H_2 production efficiency
η_{eq,H_2-ref}	equivalent H_2 production efficiency of the reference plant without capture
η_{H_2}	hydrogen production efficiency
$\eta_{th,ref}$	reference thermal efficiency of a conventional industrial boiler

plant scales. There is also widespread interest in mitigating climate change mainly by reducing the amount of CO_2 emitted to the atmosphere from large stationary sources. In the medium-to-long term, large fossil-fuel H_2 production plants fitted with CO_2 capture and storage systems (CCS) will form part of a privileged branch of technology, and therefore, R&D should be devoted to make CCS technically and commercially efficient by improving plant efficiency, reducing capital costs, and increasing the operational flexibility and reliability of hydrogen production systems.

The dominant H_2 production technology on a large scale is the steam methane reforming (SMR), which is responsible for around 50% of the hydrogen produced worldwide [6,7]. SMR comprises two reaction steps: a first reforming step operating at high temperature between 1073 and 1173 K and at high pressure using a nickel-based catalyst (reaction 1), and a second shift reaction which can be carried out either in a single stage or in two stages at different temperatures to enhance the conversion of CO to CO_2 (reaction 2). In the second case, the first shift stage is usually performed at high temperatures of 623–783 K over a chromium–iron oxide catalyst promoted by the addition of a small amount of copper (1–2 wt.%), whereas the second shift reactor operates at a lower temperature of 453–603 K over a copper–zinc catalyst so that the CO fraction is reduced to around 3 vol.% of the gas leaving the second shift reactor [6,8]. H_2 production by SMR is performed at a high pressure of around 1500–3000 kPa for the sake of economy despite its negative effect on methane conversion [8]. However, further purification steps are needed after the shift reactors to attain the high degree of H_2 purity necessary for its final use.

$$CH_4 + H_2O \leftrightarrow CO + 3H_2 \qquad \Delta H_{298\ K} = +206.2\ \text{kJ/mol} \tag{1}$$

$$CO + H_2O \leftrightarrow CO_2 + H_2 \qquad \Delta H_{298\ K} = -41.5\ \text{kJ/mol} \tag{2}$$

Although SMR is the most efficient and economic process for H_2 production on a large scale compared to the rest of the technologies in common use today such as partial oxidation, coal gasification or autothermal reforming, it has serious drawbacks [8]. The stringent conditions of high pressure and high temperature that are required in the reforming reactor as well as the high endothermicity of the reforming reaction, entail large additional fuel requirements in the reactor to guarantee the supply of the energy needed for the reforming reaction. Although the thermal efficiency of a tubular reformer and waste heat recovery section is close to 95%, the overall efficiency has been estimated to be in the range of 70–80%, when defined as the energy (on a LHV basis) of the H_2 product obtained in relation to the total LHV thermal input (natural gas and additional fuel) [6,9–11]. Efficiency can be increased if the amount of heat transferred in the tubular reformer is reduced by using a pre-reformer to decompose the large hydrocarbons before the SMR. Another option for improving efficiency is to increase the energy transferred to the reformer via a convective heat-exchange reformer (also known as gas heated reformer), where the hot product gas is cooled with the transfer of heat to the gas inside the reformer [8,12]. However, this option also entails the risk of metal dusting corrosion. Proper construction materials and the coating of exposed surfaces are required for the efficient recovery of heat from a high CO content process gas with a carbon activity higher than 1 in the 673–1073 K temperature range [13,14].

Thermodynamic constraints require the SMR to be operated at high temperatures and low pressures to facilitate high methane conversion [15,16]. However, the production of low pressure H_2 would require a subsequent compression stage before it could be used in synthesis processes or as fuel for gas turbines, which would probably make the process economically unfeasible [8]. The possibility of combining reaction and separation in order to simplify the process, enhance efficiency and improve the hydrogen yield has gained in importance. By equipping the reforming reactor with a H_2 selective membrane, equilibrium limitations can be overcome since the H_2 produced can be continuously withdrawn from the reacting gas by allowing it to permeate through the membrane. Lower operating temperatures than those required in SMR would then be possible [6,17,18]. A large number of experimental and modelling studies have been undertaken not only to demonstrate the viability of this concept but also to reduce costs and improve the design features, performance and efficiency of this technology [18–22]. One of the disadvantages of this process is that the driving force for H_2 separation is the partial pressure difference between each side of the membrane, which results in low pressure hydro-

gen production. However, when high purity H_2 is not required, for example in gas turbine applications, high feed pressures and a sweep gas on the permeate side will make hydrogen compression unnecessary [21,23–25].

An alternative to membrane reactors for enhancing the thermodynamics of the system is the sorption enhanced reforming (SER) process, which involves the addition of a Ca-based CO_2 acceptor to the commercial SMR catalyst so that the reforming, shift and CO_2 removal stages (reactions 1, 2 and 3) take place simultaneously in the reactor [15,16,26–35]. The CO_2 removal reaction yields a product gas under equilibrium conditions with a hydrogen content of around 96% (dry basis), which remains constant over a wide temperature range from 923 K to 1023 K. This temperature range is well below that required for a conventional catalytic SMR process, eliminating the need for expensive and troublesome tubular reformer reactors and favouring the use of cheaper materials and heat exchanger equipments [15,16,29,36]. A shift catalyst is not required in the SER process since the shift reaction is favoured by the removal of CO_2, making the SER much simpler than SMR. In the SER process, the heat released by the shift and the CaO carbonation reactions balances the energy required by the endothermic reforming process, and therefore no external heating is required by the reforming reactor.

$$CaO + CO_2 \leftrightarrow CaCO_3 \qquad \Delta H_{298\ K} = -178.8\ kJ/mol \tag{3}$$

However, to ensure continuous operation, the $CaCO_3$ formed by the CO_2 removal reaction must be regenerated in a second reactor (named calciner) to enable it to be cyclically used. This regeneration is highly endothermic and requires external energy to provide heat for calcination. It has been widely proposed that the energy for regeneration could be supplied by the direct combustion of additional fuel in the calciner or regenerator [37–39], although indirect heating by heat exchangers using a portion of the recycled gas heated by additional fuel combustion has also been proposed [15,16,28,40]. Another alternative is the zero emission gas (ZEG) concept, which is based on coupling the SER reactor to a solid oxide fuel cell (SOFC) so that the high-temperature waste heat produced in the SOFC is used by means of an indirect heat exchange system to perform the endothermic calcination process at a temperature of around 1173 K [41]. This concept seems promising in the medium-to-long term as long as the technical challenges related to the heat transfer loop and SOFC materials can be solved. Other alternatives include the lime enhanced gasification (LEGS) process, which allows coal gasification to be carried out in the presence of a Ca-based sorbent and thereby enhances the hydrogen yield. Energy for the regeneration of the sorbent is supplied by burning the remaining char with oxygen and by the exothermic oxidation of CaS to $CaSO_4$, both of which come from the gasification step [42]. An additional alternative is to use a chemical looping combustion system to supply energy to regenerate the Ca-based sorbent. This method was originally proposed by Lyon [43] for fuel combustion, but later the concept was adapted to become part of the unmixed reforming (UMR) concept [44,45], in which a Ni/NiO chemical loop is used to provide energy for calcination. In this process, the Ni-based solid acts as catalyst in the reforming stage, and during the sorbent regeneration step air is passed through the solid bed to oxidize the metal. The energy released in the oxidation reaction is absorbed by the $CaCO_3$ calcination reaction, and the CO_2 captured during the SER step is released [46]. In this way, an efficient transfer of energy occurs between the oxidation and calcination reactions. The drawback is that the CO_2 released in the calciner is diluted with N_2 from the air used for metal oxidation making CO_2 capture no longer feasible.

The process discussed in the present work is based on the UMR concept but it makes use of a Cu/CuO chemical loop to supply heat for regeneration of the sorbent using the energy released in the CuO reduction process [47,48]. The sequence of reaction stages in this novel concept is shown in Fig. 1. It is performed in a series of fixed bed reactors where pressure and temperature are modified to favour the production of hydrogen while producing at the same time a concentrated stream of CO_2 suitable for purification, compression and storage. The first step (stage A in Fig. 1) comprises the production of H_2 through a SER process operating at high pressure with steam and natural gas (NG) as feedstock in the presence of a Ca-based sorbent, a Ni-based reforming catalyst and a Cu-based material, all in their reduced form. The Ni- and Cu-based materials remain unchanged in this step and the formation of $CaCO_3$ enhances the H_2 production equilibrium (the sum of reactions 1, 2 and 3). In the next step (stage B), oxidation of the Cu-material takes place when pressurised diluted air is fed in under conditions of a limited oxidation rate and minimal $CaCO_3$ decomposition. In the last process step (stage C), the calcination of the $CaCO_3$ formed in the SER stage takes place thanks to the heat released from the oxidation of CH_4, CO or H_2 resulting from the reduction of CuO. A suitable Cu/CaO molar ratio must be chosen to ensure that the heat released in the CuO reduction is enough to sustain the endothermic $CaCO_3$ calcination step. A full conceptual design of this novel process, assuming ideal plug flow models for each reactor [49], as well as a dynamic pseudo-homogeneous model for a fixed bed reactor operating in the SER stage of this process have been recently published [50]. A reasonable operating window has been established to ensure that the SER stage of the Ca/Cu process will attain equilibrium. Lower space velocities than in conventional steam reforming are required for carbonation to proceed correctly [51]. There is growing interest in developing composite CaO–CuO materials suitable for this Ca/Cu looping process [52–56]. The objective of these new materials is to reduce the amount of support material that acts as thermal ballast in the solid bed. Promising results for the performance of this composite under the Ca/Cu looping process conditions have been reported, contributing to the acceptance of this concept as part of pre-combustion CO_2 capture strategy. Moreover, in a previous work, it has been demonstrated that this novel concept is a suitable technology for being integrated with a natural gas combined cycle to produce power, with efficiency penalties of around 8 points, similar to those obtained with other emerging and commercial technologies such as chemical absorption [57].

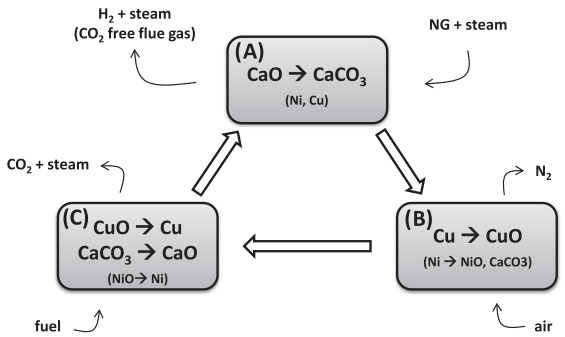

Fig. 1. Conceptual scheme of the Ca/Cu looping process for hydrogen production.

The concept assessed in this work has many similarities with packed-bed chemical looping process (CLC) systems studied in recent works [58–64]. These works explored theoretically and experimentally the feasibility of the CLC concept in a high temperature fixed-bed system. These works show that the gas/solid reactions involved can proceed very rapidly in narrow reaction fronts, which would allow an effective cyclic operation in a system composed by several dynamically operated fixed-bed reactors. This system is hence capable of generating hot gas products with stable temperature and flow rate, suitable for application in a power plant.

Advantages of packed beds over fluidised beds in CLC lie in the non-need of high temperature-high pressure filtering of entrained particles before the gas turbine and of the non-need of circulating hot solids between pressurised reactors, which has not been demonstrated yet. On the other hand, more complex heat management strategies and a larger number of reactors with valves operating with hot gases are needed with packed beds, whose feasibility should be assessed from an economic point of view. As far as valves are concerned, it can be highlighted that some manufacturers already offer high temperature valves operating at the temperatures considered in this work and the development of valves suitable for this application can be expected in a medium-term horizon required for the scale up of this concept [65].

In the present work, the main objective is to develop a detailed and comprehensive process design of a H_2 production plant based on the Ca/Cu looping process described above. Reasonable assumptions concerning NG processing and the reactions involved in each stage of the process have been made, and an Aspen Hysys simulation model of the entire plant has been assembled. To make a thermodynamic assessment of the entire plant, a complete energy integration study involving all the gas streams has been proposed, in which the advantages and drawbacks of the process are highlighted. The results obtained have been compared with those achieved by other reference hydrogen production plants based on commercial reforming technology with and without CO_2 capture.

2. Process description

The assumptions made in this work are based on the three main process units that form the basis of the H_2 production plant under study: (i) NG treatment, (ii) the H_2 production process, and (iii) the H_2 purification unit. The mass and energy balances used in this work to solve the different reaction stages of the H_2 production process are based on those reported by Fernández et al. [49], and adapted to the assumptions of this study. Fig. 2 illustrates the different units considered to construct an Aspen Hysys simulation model of a H_2 plant based on the Ca/Cu looping process. The following sections describe in detail the main process units cited above.

2.1. Sulphur removal and pre-reforming of natural gas

The reforming catalyst is extremely sensitive to sulphur and, therefore, it is necessary to remove all the sulphur compounds before reforming in a non-regenerative ZnO-based solid bed. To enhance the reactivity of ZnO towards sulphur compounds, it is necessary to convert the compounds into hydrogen sulphide (H_2S) which is more reactive towards ZnO than organic sulphur compounds. The formation of H_2S takes place by hydrogenation in a catalytic bed of cobalt and molybdenum oxides deposited on an alumina base, which can be placed either in a separate vessel or as a layer on top of the ZnO bed. Hydrogenation takes place at temperatures not higher than 613–643 K so as not to damage the alumina substrate [66], using a H_2 concentration of 2–5 vol.% to ensure that hydrogenation formation proceeds at a sufficient rate [67]. The ZnO bed usually operates at the same temperature as that required for the hydrogenation step. Since equilibrium is usually reached, it is possible to reduce the sulphur content to below 0.1 ppm [66]. As the presence of steam inhibits H_2S retention, NG is usually mixed with steam after S-removal (see Fig. 2). Depending on the pressure of the downstream process and the characteristics

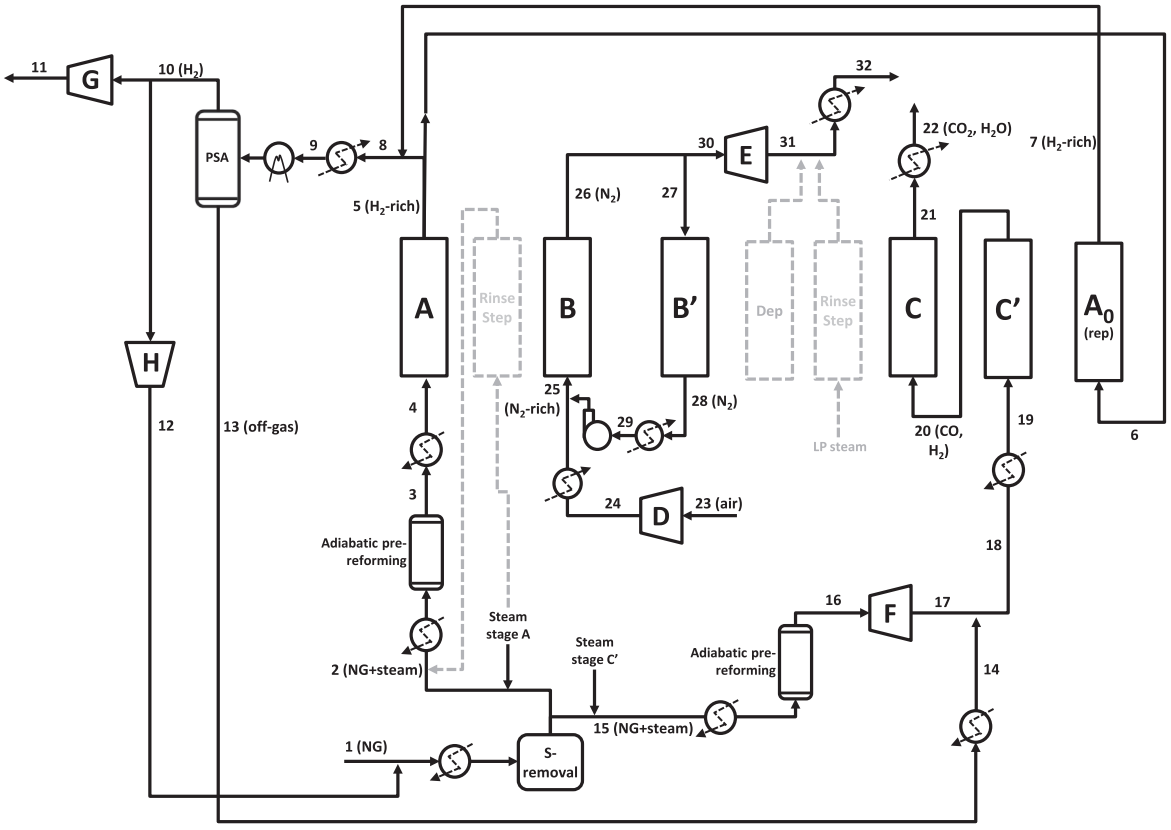

Fig. 2. Simplified layout of the assessed H_2 production plant based on the Ca/Cu looping process (A, B and C are the reaction stages of the H_2 production process as referred to in Fig. 1; D is the air compressor; E and F are gas expanders, and G and H are H_2 compressors).

of the whole plant, steam can be bled from a steam turbine or generated by recovering heat from the process streams.

At the high temperatures reached in the reforming steps of the Ca/Cu looping process, the decomposition of higher hydrocarbons via thermal cracking into olefins, and then into coke, is likely to occur [68]. Moreover, at high temperature, the lower the steam-to-carbon (S/C) molar ratio in the inlet gas, the greater the risk of formation of whisker carbon, which has a high mechanical strength and can cause the breakup of catalyst particles or the reduction of the active catalyst surface, and therefore, its subsequent deactivation [8]. In the layout proposed (Fig. 2), NG is pre-reformed before it enters the H_2 production process, to decompose higher hydrocarbons into CH_4 and CO, according to reactions 2, 4 and 5. The steam reforming of higher hydrocarbons (reaction 4) is usually considered as irreversible for all higher hydrocarbons provided that catalytic activity is strong enough. At the same time, equilibrium between methanation (5) and water gas shift reaction (2) is established [69].

$$C_nH_m + nH_2O \rightarrow nCO + \left(n + \frac{1}{2}m\right)H_2 \qquad \Delta H_{298\ K} > 0 \tag{4}$$

$$CO + 3H_2 \leftrightarrow CH_4 + H_2O \qquad \Delta H_{298\ K} = -206.2\ \text{kJ/mol} \tag{5}$$

Pre-reforming is commonly carried out in an adiabatic fixed bed reactor at a temperature between 653 and 773 K in the presence of a Ni-based catalyst [68]. This pre-reforming step is performed after S-removal to avoid H_2S being chemisorbed on the nickel surface. Although pre-reforming occurs after the S-removal unit, sulphur traces will be retained by the pre-reforming catalyst and will slowly poison the nickel catalyst. However, this will ensure a virtually sulphur-free gas for the H_2 production process and result in a prolongation of the downstream solids life: the reforming catalyst, Ca-based sorbent and Cu-based material. In NG adiabatic pre-reformers, the temperature decreases because of the endothermicity of steam reforming of higher hydrocarbons, which allows the equilibrium from reactions 4 and 5 to be established at a lower temperature than at the inlet. An even more efficient option for pre-reforming than the adiabatic one described is that offered by a gas heated pre-reformer where high temperature reformed syngas is put into contact with the NG-steam charge. Pre-reforming reactions then occur at a higher temperature than with the adiabatic option, favouring a higher CH_4 reforming reaction and improving heat recovery [12]. An additional advantage in this case would be the low-CO content of the streams to be cooled, which would prevent any risk of metal dusting in the gas heated reformer. For the present work, the gas heating option was discarded because the heat obtainable from the hot sources would be insufficient to sustain the process. An adiabatic pre-reforming system was chosen instead.

In the layout proposed for the Ca/Cu looping process (see Fig. 2), NG is fed into the process at high pressure and ambient temperature (stream 1). It is then mixed with a slip of compressed H_2 (stream 12) to obtain a concentration of H_2 of around 2 vol.%, which is preheated up to 638 K and then fed into the S-removal unit. Afterwards, the mixture splits into the NG to be fed in at stage A, and the NG to be fed in at stage C′ of the Ca/Cu looping process. Each stream is mixed with the necessary amount of steam to reach the required S/C molar ratio, and is then fed into the corresponding adiabatic pre-reformer.

2.2. H_2 production process

The H_2 production process in this study is based on the three reaction steps explained briefly in the introduction. Mass and energy balances for the dynamically operated adiabatic fixed-bed reactors, as well as the operating window for each step have been illustrated in detail by Fernandez et al. [49]. In the present work additional process assumptions have been made concerning the raw material used, solids involved and reactions that occur at each step. These assumptions contribute substantially to the detailed and complete scheme of this novel H_2 production process depicted in Fig. 2. Table 1 summarises the main assumptions for the simulation of the heat and mass balances of this H_2 production plant.

CaO hydration could occur due to the presence of a high excess of steam during the operation, especially in the reforming stage A. Traditionally, hydration has been proposed as a reactivation method to improve the performance of CaO as a regenerable sorbent in Ca-looping systems [70–73]. Usually, CaO hydration is tested at temperatures lower than 673 K because $Ca(OH)_2$ is unstable above this value at atmospheric pressure [74]. Moreover, in conventional Ca-looping systems there is no interest in working under high pressures that would necessarily lead to higher capital and operating costs [75]. However, in this work, high pressure is used in stages A, B and B′, while maximum temperatures may range between 923 and 1143 K, depending on the input conditions selected [49,51]. Curran et al. [76] studied the phase equilibrium in two binary systems, CaO–$Ca(OH)_2$ and $Ca(OH)_2$–$CaCO_3$, at elevated pressures and temperatures, and determined the chemical properties of the Ca-based CO_2 sorbents. Equilibrium data revealed the formation of melts at temperatures of around 1088 K, whenever the steam partial pressure exceeded the critical value of 1300 kPa. Paterson et al. [77] also observed melt formation, but at higher temperatures (1283 K). Fuerstenau et al. [78] presented equilibrium liquid curves for the CaO/$Ca(OH)_2$/$CaCO_3$ ternary system and showed that melts could contain around 60% of $CaCO_3$ at 7000 kPa and 1053 K. These results demonstrate that the formation of melts from hydrated CaO can theoretically reactivate spent Ca-based sorbents, as reported in the literature for some processes. In the CO_2 acceptor process [76,77] and in the HyPr-RING process [79,80], a Ca-looping system is integrated in a gasification scheme in order to obtain a high H_2 yield from coal. The hydration of the Ca-based sorbents at high pressure and temperature was observed to improve the durability of the sorbent after several carbonation/calcination cycles, even under the eutectic conditions. However, there is a lack of knowledge concerning the consequences of possible agglomeration phenomena resulting from the melted material and how the presence of hydrated sorbent might affect the SER equilibrium reactions, and consequently the H_2 yield. Furthermore, it has been demonstrated that the beneficial hydration effects on carbonation conversion disappear if the hydrated sorbent is subjected to temperatures above 973 K [81]. In this study, the operating conditions for carrying out the SER stage (A in Fig. 2) were chosen with the aim of avoiding CaO hydration.

Equilibrium data reported in the literature for the CaO hydration reaction at high temperatures [74,82], were employed to produce Fig. 3. The most critical conditions for CaO hydration in the Ca/Cu looping process correspond to stage A and the following rinse step, which are the points of highest steam partial pressure. SER stage A is slightly exothermic and the gas temperature throughout the reactor increases from $T_{gin,A}$ to a maximum value of $T_{max,A}$. As can be seen in Fig. 3, the equilibrium steam pressure increases with temperature, and thus it will be necessary to go to higher temperatures to avoid CaO hydration when using high steam pressures for the gas fed in at stage A. However, the carbonation reaction is necessary at this stage for CO_2 removal from the gas phase to occur and, therefore, excessively high temperatures will have a negative effect on the carbonation reaction. Moreover, the pressure must not be too low since the H_2 compression that follows (unit G in Fig. 2) contributes to increase the power required for the entire plant. As a trade-off between these conflicting demands, inlet conditions of 973 K and 1500 kPa were considered

Table 1
Summary of the assumptions made to construct the simulation model of the H_2 production plant based on the Ca/Cu looping system.

Natural gas	
Composition	89% CH_4, 7% C_2H_6, 1% C_3H_8, 0.11% C_4H_{10}, 2% CO_2, 0.89% N_2
LHV	46.482 MJ/kg
NG distribution conditions	288 K/1900 kPa
Ca/Cu chemical looping process	
Catalyst composition	18 wt.% NiO over Al_2O_3
Ca-sorbent composition	85 wt.% CaO over Al_2O_3 (40% of active CaO)
Cu-based material composition	65 wt.% Cu over Al_2O_3
Amount of catalyst used	0.3 g catalyst/g of CaO in the sorbent
Superficial gas velocities in stages A/B–B′/C–C′	0.5/1–2/5–6 m/s
O_2 concentration in stage B	3.4 vol.%
Maximum temperature in oxidation stage	1103 K
Maximum temperature in calcination/reduction stage	1143 K
S/C molar ratio in stage C′	1
Sulphur removal unit	
Operating temperature	638 K
Adiabatic pre-reformers	
Gas inlet temperature	763 K
Operating pressure	1600 kPa
Pressure drop	36 kPa
Booster air compressor	
Polytropic efficiency	85%
Mechanical-electric efficiency	94%
Auxiliary fan and H_2 compressor	
Polytropic efficiency	80%
Mechanical-electric efficiency	94%
N_2-rich expander	
Polytropic efficiency	85%
Mechanical–electric efficiency	94%
Pre-reformed NG expander	
Polytropic efficiency	80%
Mechanical–electric efficiency	94%
Steam turbine	
Polytropic efficiency	80%
Mechanical–electric efficiency	94%
Heat recovery system	
Minimum ΔT in gas–liquid heat exchangers	20 K
Minimum ΔT in gas–gas heat exchangers	25 K
Minimum ΔT in gas-boiling liquid heat exchangers	10 K
Heat loss in each heat exchanger	0.7% of heat transferred
Total pressure drop in NG pre-heating	300 kPa
Total pressure loss in cooling gas streams	7% of the initial pressure
Evaporation pressure	1600 kPa
CO_2 compressor	
Number of intercooled compression stages	5
Inter-cooling temperature	301 K
Inter-cooling pressure loss	1%
Outlet pressure after compression stages	8900 kPa
Final pumping CO_2 exit pressure	11,000 kPa
Polytropic efficiency of compression stages	84%
Pump hydraulic efficiency	80%
Mechanical–electric efficiency	94%

to be reasonable for the gas stream fed in at stage A (black dot highlighted in Fig. 3). Under these conditions for the gas fed in at stage A, the maximum temperature in the bed at the reaction front $T_{max,A}$ will be at around 1035–1050 K depending on the S/C ratio chosen, which will result in an active CaO conversion of 78–85% and a H_2 yield at equilibrium conditions of at least 91 vol.% (dry basis). To achieve SER equilibrium conditions in this stage, as the carbonation reaction rate is much lower than that of the reforming and shift reactions, a low superficial gas velocity of around 0.5 m/s was chosen for stage A [51].

To avoid the unwanted combustion of any hydrogen remaining in the solid bed during the subsequent stage B, and to avoid hydrogen being vented to the atmosphere which would have a negative effect on the overall hydrogen yield of the process, a rinse step has been introduced between stages A and B, as depicted by the grey dashed lines in Fig. 2. High pressure steam at 1600 kPa and 973 K was used for cleaning on the assumption that five reactor volumes is a proper value for a complete rinse. It should also be noted that the amount of steam used for rinsing does not have any relevant effect on the plant's performance. As a matter of fact, after rinsing, the steam is recycled to contribute to the S/C molar ratio in stage A and will be fed in before the adiabatic pre-reforming in order to enhance the CH_4 conversion (as indicated in Fig. 2).

The oxidation stage in the Ca/Cu looping process (stage B in Fig. 2) operates at the same pressure as in stage A to enable the non-recycled N_2 (stream 30 in Fig. 2) to be sent to an expander for power generation (unit E in Fig. 2). As Cu oxidation is highly exothermic (reaction 6), the maximum temperature ($T_{max,B}$) needs to be strictly controlled to avoid any non-desirable reactions of Cu, the loss of CaO active surface and to prevent the calcination of

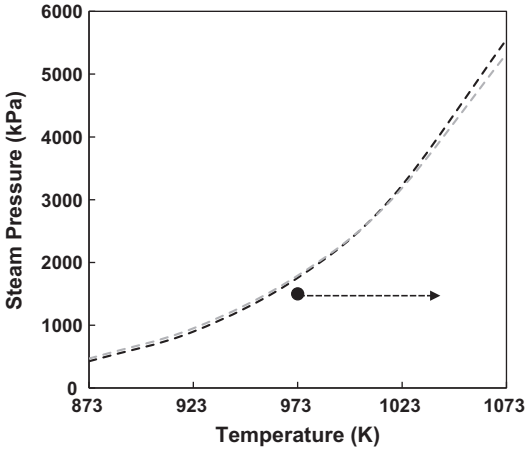

Fig. 3. CaO hydration equilibrium (data from Samms and Evans [69] (grey line) and Lin et al. [61] (black line)).

$CaCO_3$. Reasonable values for $T_{max,B}$ range between 1103 and 1143 K, where the maximum CO_2 production resulting from the calcination of $CaCO_3$ is moderate and determined by the CaO/$CaCO_3$ equilibrium. Since the lower the temperature, the lower the CO_2 loss, a 1103 K $T_{max,B}$ has been assumed. According to the values given by Barker [83] for the carbonation equilibrium, maximum CO_2 partial pressure in the gas exiting stage B (stream 26 in Fig. 2) will be 36 kPa at 1103 K, which corresponds to a CO_2 content of around 2.4 vol.%.

$$Cu + 1/2\,O_2 \rightarrow CuO \qquad \Delta H_{298\ K} = -156.1\ kJ/mol \tag{6}$$

To moderate the $T_{max,B}$ reached at this stage and avoid hot spots that could damage the solid material in the reactor, the oxidation rate must be controlled by reducing the temperature and the O_2 concentration in the gas fed in at stage B (stream 25 in Fig. 2). Gas temperatures in the range of 423–573 K and an O_2 concentration of around 3–4 vol.% serve to limit $T_{max,B}$ to 1103 K [49]. This low O_2 concentration is achieved by recycling a large fraction of the O_2-depleted gas exiting stage B (stream 27 in Fig. 2) and mixing it with the compressed air at 1500 kPa coming from an air compressor (unit D in Fig. 2).

When stage B has finished and all the Cu-based material has been oxidised to CuO, the solid bed is at the gas inlet temperature ($T_{gin,B}$), which makes it impossible to perform the next reduction/calcination stage C. To allow stage C to occur, before carrying out the depressurization of the solid bed, a heating stage B′ is included in order to transfer the excess heat in the recycled gas to the solid material in the fixed bed. Due to the non-uniform temperature at the beginning of stage B, during this stage gas is sequentially produced at the two temperatures $T_{max,A}$ and at $T_{max,B}$. Depending on the recirculation ratio chosen (molar flow rate of stream 27 to molar flow rate of stream 26, Fig. 2), the proportion of gas at $T_{max,A}$ and at $T_{max,B}$ at the stage B outlet will vary, and therefore the temperature reached during the heating stage B′ will also change. In any case, the gas exiting stage B′ will be hotter than the required temperature $T_{gin,B}$ and it will need to be further cooled down. After cooling, a blower is introduced to compensate for the gas pressure losses in stages B and B′, and in the heat exchangers. A recirculation ratio of around 0.85 for all the operating conditions examined in this work was obtained from the mass and energy balances to ensure a proper control of $T_{max,B}$. The superficial gas velocity in stages B and B′ was set at around 1.5–2 m/s so as not to incur excessively high pressure losses [49]. This velocity leads to a pressure drop of around 25–50 kPa in each stage that, together with the pressure loss in the heat exchangers, adds up to a total pressure drop for the recycled O_2-depleted gas (stream 29 in Fig. 2) of around 200 kPa. As will be seen in Section 4.2, the energy consumed by the blower is relatively high and affects the efficiency of the process considerably.

Once stage B′ has finished, the pressure must be reduced to atmospheric level so that the next calcination/reduction reaction stage can proceed. The solid bed is depressurised on the product side, and the N_2-rich gas swept from this stage is mixed with the expander outlet gas for cooling before being sent to the stack. After depressurisation, a rinse step is introduced using low pressure steam at around atmospheric pressure to clean away any possible traces of gas present in the system. The steam required for rinsing can be generated at a pressure slightly higher than atmospheric pressure, thanks to the low temperature heat available in the process (i.e. before the condenser of the H_2-rich gas or in the intermediate cooling stages in the CO_2 compressor). Also, due to the large availability of low temperature heat, the amount of steam used for this rinse step does not appreciably affect the overall performance of the plant. After rinsing, steam, still at a high temperature, is sent to the expander outlet for purposes of heat recovery.

The next reaction stage in the process is the calcination of the $CaCO_3$ formed during the SER stage together with the simultaneous reduction of the CuO formed in stage B. The Cu/CaO molar ratio chosen for the solid bed should be such that stage C is thermally neutral, and the heat released by the reduction of CuO is equivalent to the energy required for the $CaCO_3$ calcination. As proposed by Fernández et al. [49], CuO reduction is carried out by feeding into stage C a mixture of the CO/H_2 produced in the subsequent reforming stage C′, according to reactions 7 and 8. Traces of CH_4 are present in the mixture of CO/H_2 generated in stage C′ that reduce CuO according to reaction 9. The pressure in stage C will need to be reduced to atmospheric level to allow calcination at reasonable temperatures. Temperatures in stage C above 1123 K are needed to decompose the $CaCO_3$. The drawback is that, this step requires a large supply of Cu to the overall process, and consequently of NG, to heat the solid bed up from the temperature in stage B′ to that required by stage C. Moreover, temperatures greater than 1173 K may cause the deactivation of CaO due to sinterization and undesired Cu reactions [84]. For these reasons, the temperature in stage C was set to 1143 K in this work, leaving a margin of around 20 K over the calcination equilibrium temperature, to ensure sufficiently high calcination kinetics.

$$CuO + CO \rightarrow Cu + CO_2 \qquad \Delta H_{298\ K} = -131.9\ kJ/mol \tag{7}$$

$$CuO + H_2 \rightarrow Cu + H_2O \qquad \Delta H_{298\ K} = -89.6\ kJ/mol \tag{8}$$

$$4CuO + CH_4 \rightarrow 4Cu + CO_2 + 2H_2O \qquad \Delta H_{298\ K} = -195.3\ kJ/mol \tag{9}$$

As shown in Fig. 2, pre-reformed NG is fed into stage C′ to perform an additional steam methane reforming step while the solid bed temperature is reduced to 973 K for the start of a new cycle. In this way, heat from the cooling of the bed is efficiently recovered as chemical energy by steam reforming reaction, providing a CO–H_2 rich gas for the following C step, thereby reducing the amount of NG required to regenerate the sorbent. In order to favour steam reforming in stage C′ and to avoid carbon deposition on the reduced bed at the entrance during stage C, a S/C ratio of 1 was selected, which is a much lower value than for stage A since the promotion of steam reforming is not of primary importance here. The pressure in stage C′ is atmospheric, and the pre-reformed gas must be expanded from 1600 kPa to near atmospheric pressure (in unit F depicted in Fig. 2), and heated up to the established temperature $T_{gin,C'}$ before stage C′. The gas temperature at the inlet to stage C′ must be 973 K, the same as that in stage A, to prevent the solid bed cooling down to below this temperature and then fa-

vour CaO hydration during subsequent stage A. H_2-rich gas from stage A is sent to a pressure swing adsorption (PSA) unit for purification where an off-gas (mainly H_2, CH_4 and CO) at near atmospheric pressure is produced. This off-gas is fed into stage C′, together with the pre-reformed NG, to reduce the consumption of NG and emissions of CO_2 resulting from the combustion of the PSA off-gas. The superficial gas velocities in stages C and C′ were considered to be around 5–6 m/s since there are no restrictions from the reforming and CuO reduction kinetics in these stages.

Reducing the amount of NG fed into stage C′ by using the PSA off-gas leads to an excess of heat in the solid bed at the end of stage C′. As a result, an additional step is included (stage A0 in Fig. 2) to remove the excess of heat from the bed and to set the temperature to 973 K for a new cycle. It is proposed that a fraction of the H_2-rich gas from stage A, which is at around 1500 kPa and at the desired temperature of 973 K, is introduced into stage A0. Moreover, solid bed pressurisation occurs during stage A0 due to the H_2-rich gas from stage A being at the desired pressure, and no additional pressurisation stages are therefore necessary. The H_2-rich gas from stage A is at equilibrium conditions at $T_{max,A}$, and contains mainly H_2 and steam. When part of this gas is fed into stage A0, the solid bed will cool down mainly due to an exchange of sensible heat between the gas at 973 K and the solid material at $T_{max,C}$. However, there will be an additional cooling by the reforming of the small amount of CH_4 in the gas phase that is going to be heated up to a $T_{max,C}$ of 1143 K. As the carbonation reaction is not substantially favoured at 1143 K (the carbonation equilibrium constant is 1.53 atm^{-1}, according to Barker [83]), and due to the fact that the superficial gas velocity chosen for this stage will be too fast for the carbonation equilibrium to occur [51], $CaCO_3$ formation in stage A0 can be ignored. Once stage A0 has finished, the H_2-rich gas leaving this stage at $T_{max,C}$ is mixed with the non-recycled H_2-rich gas leaving stage A at a $T_{gin,A}$ of 973 K, and the mixture (stream 8 in Fig. 2) is cooled down to around 303 K, ready to be introduced into the PSA unit. The heat recovered from this cooling step is used to preheat the gas streams and produce steam, as described in Section 3 below.

To better clarify the temperature evolution of the gas from each stage, table 2 is included, where the temperature of the bed at the different stages and the temperature of the gas generated from each stage in the cases assessed in this work are reported. For a detailed discussion on how these temperatures are generated, the reader is addressed to [49]. Since the process simulation code performs steady state simulations, a proper average temperature has been used in the simulations for the gas streams produced at non-constant temperatures. It should also be highlighted that, due to kinetics and heat transfer limitations, in a real reactor the heat and reaction fronts will not be perfectly defined as in an ideal situation. As more accurate 1D modelling also shows [50,51,60], some dispersion of temperature and chemical species in the axial direction occurs so that temperature and composition of gases at reactor outlet gradually change with time. This effect, which can lead to gas leakages or to incomplete utilization of the bed material, has also been neglected in this work and needs to be further explored with modelling and experiments.

The Ni-based reforming catalyst introduced into the process affects the mass and heat balances, since the operating conditions in stage B and stage C favour its oxidation and reduction, with O_2 and H_2 being consumed respectively. This also contributes to the energy balance due to the high exothermicity of the oxidation reaction (−470.8 kJ/mol at 1123 K). Moreover, the reforming catalyst and the inert support of the Ca and Cu functional materials act as thermal ballast and require energy to be heated up to the maximum temperature of $T_{max,C}$. Therefore, a higher amount of Cu-based material is needed in the process. To account for these effects, Ni-catalyst oxidation and reduction reactions are included in the mass and energy balances solved for each stage of this process. A typical Ni-based reforming catalyst supported over Al_2O_3 with an active phase of 18 wt.% has been adopted for the purpose of this work.

2.3. H_2 purification unit

H_2-rich gas from stage A of the Ca/Cu looping process is sent to a PSA unit for purification. The PSA unit represents state-of-the-art technology for both gas separation and purification. It is based on the use of regenerable solid sorbents packed in different columns, which selectively adsorb certain gas components from a gas mixture [85]. This technique operates at ambient temperature and high pressure, and delivers a gas stream enriched in those components that have been less adsorbed into the solid from the gas mixture, at a pressure close to that of the feed gas (around 50 kPa lower than the feed pressure) [86]. Traditionally, this purification technique has been used in the SMR process to produce H_2 with a purity of up to 99.999% [6,36,87], from a typical gas mixture composition (dry basis) of 76% H_2, 17% CO_2, 4% CH_4 and 3% CO. Un-

Table 2
Gas and solid temperatures associated to different stages for the assessed cases.

	Stage A	Stage B	Stage B′	Stage C	Stage C′
Ni catalyst, S/C = 4					
Initial bed temperature (K)	973	973/1049	473	1049/1103	1143
Final bed temperature (K)	973/1049	473	1049/1103	1143	973/1143
Maximum temperature (K)	1049	1103	1103	1143	1143
Inlet gas temperature (K)	973	473	1049/1103	1143	973
Outlet gas temperature (K)	973	1049/1103	473/1049	1103	1143
Average outlet gas temperature (K)	973	1059	650	1103	1143
Ni catalyst, S/C = 3					
Initial bed temperature (K)	973	973/1036	473	1036/1103	1143
Final bed temperature (K)	973/1036	473	1036/1103	1143	973/1143
Maximum temperature (K)	1036	1103	1103	1143	1143
Inlet gas temperature (K)	973	473	1036/1103	1143	973
Outlet gas temperature (K)	973	1036/1103	473/1036	1103	1143
Average outlet gas temperature (K)	973	1063	649	1103	1143
Pt catalyst, S/C = 4					
Initial bed temperature (K)	973	973/1039	473	1039/1113	1143
Final bed temperature (K)	973/1039	473	1039/1113	1143	973/1143
Maximum temperature (K)	1039	1113	1113	1143	1143
Inlet gas temperature (K)	973	473	1039/1113	1143	973
Outlet gas temperature (K)	973	1039/1113	473/1039	1113	1143
Average outlet gas temperature (K)	973	1063	628	1113	1143

der these conditions, the usual H_2 recovery efficiency is around 90% [87]. Operating parameters that influence the H_2 recovery rate in PSA systems include temperature, pressure and composition of the gas feed, but the most influential parameters affecting H_2 recovery are the pressure of the feed and the off-gas: the higher the ratio of the feed to off-gas pressure, the higher the H_2 recovery rate and, therefore, the lower the investment costs for a given product rate [86]. A pressure ratio between the absolute feed pressure and the off-gas (or waste gas) pressure of at least 4 is required to ensure a reasonable H_2 recovery rate of around 70–75%. Although a pressure ratio of more than 15 does not improve the H_2 recovery, it will lead to an increase in the energy consumption required to reach a higher operating pressure, and to around 90% of the H_2 fed into the PSA being recovered as a high-purity product [86]. It seems reasonable to expect a higher H_2 recovery rate under SER conditions of a high H_2 concentration at the inlet of the PSA unit (a maximum of 96% of H_2, on a dry basis, when SER is performed at 923 K) [15,36]. However, such a scenario has not yet been analysed in the literature. Moreover, the presence of N_2 in the NG used to produce the H_2-rich gas introduced in the PSA affects the H_2 purity since the affinity of the materials towards N_2 is usually small. Some PSA applications permit N_2 removal from NG such as the Molecular Gate™ PSA process (based on a synthetic titanosilicate EST-4) [85], which allows the purity of H_2 to be enhanced. In this work, the PSA unit is assumed to operate at a temperature of around 303 K and around 1500 kPa, with an off-gas pressure close to atmospheric pressure and a H_2 recovery of 90%.

3. Heat recovery system design

A heat recovery system has been designed in this study to allow the input stream temperature to be adapted to the specifications of each stage and the steam flow rate to be maximised for stages A and C′ of the Ca/Cu looping system. Fig. 4 shows a schematic layout of the heat recovery system designed in this work. The temperatures shown in this figure correspond to those of the highest H_2 yield case (S/C of 4 in stage A) but similar values are obtained using different S/C ratios, which means that the same heat recovery arrangement can be adopted in the other cases.

The boiler feedwater is assumed to enter into the plant at 600 kPa and 423 K and, after reaching 1600 kPa, it passes through an economiser and an evaporator to be slightly superheated at 523 K. After passing through these units, the steam is split into two streams, mixed with the desulphurised NG before the pre-reformers and then, after the pre-reformers, charge is fed into stages A and C′ of the Ca/Cu looping system. In the previous description of the Ca/Cu looping system, reference was made to the following hot gas streams that could be used for heat recovery in gas pre-heating and/or steam generation:

1. H_2-rich gas at 995 K (stream 8 in Figs. 2 and 4) resulting from the mixing of non-recycled H_2-rich gas from stage A at 973 K and recycled H_2-rich gas from stage A0 at $T_{max,C}$. This stream is cooled down to near ambient temperature (303 K in this work) and then fed into the PSA unit.
2. CO_2-rich stream exiting stage C at $T_{max,B}$ (stream 21) that is cooled down to near ambient temperature, dried and pumped up to 110 bar for storage.
3. O_2-depleted gas stream from stage B′ at $T_{max,A}$ (fraction of stream 28) which must be cooled to $T_{gin,B}$ before being fed into stage B.
4. Compressed air at 690 K (stream 24) to be fed into stage B at $T_{gin,B}$.
5. O_2-depleted stream at 592 K after it has been expanded in unit E of Fig. 2 (stream 31).

As a consequence of the feedwater temperature chosen at the economiser outlet (463 K) and the minimum temperature difference of 20 K between the gas and liquid in the heat exchanger considered in this work (see Table 1), the temperature of the recycled gas, after it has passed through the economiser and the evaporator

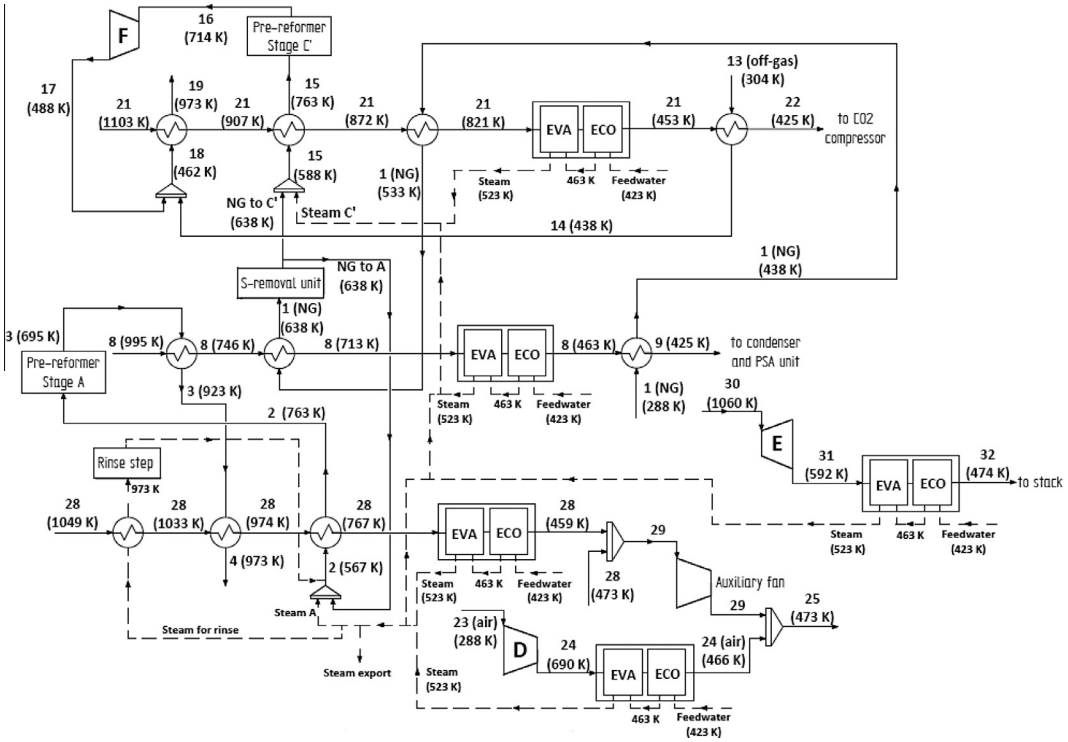

Fig. 4. Layout of the heat recovery system proposed in this work (the process stream numbers refer to those in Fig. 2; Notation used: EVA: evaporator; ECO: economiser).

(stream 29 in Figs. 2 and 4), is around 468 K. A similar temperature results from the cooling of the compressed air exiting unit D in Fig. 2. Consequently, the temperature of the gas fed in at stage B (stream 25 in Figs. 2 and 4), which results from mixing stream 24 and stream 29, is around 473 K (=$T_{gin,B}$). The temperature, pressure, flow rate and composition of the main flows of the Ca/Cu plant, when operating under the conditions necessary to achieve the highest H_2 yield (S/C = 4), are reported in Table 3 according to the notation used in Fig. 2.

As shown in Fig. 4, NG enters the system at 288 K and 1900 kPa (to compensate for the pressure loss in the pre-heating steps, the S-removal unit, and the adiabatic pre-reformer), and it is heated up to the S-removal temperature of 638 K with heat from stream 8 and stream 21. Once it exits the S-removal unit, the NG is split into two streams, which are sent to stages A and C′ respectively. Both NG streams are mixed with steam at 523 K and 1600 kPa, in proportions that they satisfy the S/C ratio required. As mentioned in Section 2.2, the steam flow needed for the rinse step between stages A and B is recycled and mixed to the NG stream before the pre-reformer. This mixture (stream 2), which is around 567 K, is heated up to the pre-reformer temperature of 763 K thanks to the heat recovered from stream 28. The charge at 695 K after the adiabatic pre-reformer (containing H_2O, CH_4, H_2, CO_2 and traces of CO) is heated in two stages up to the required temperature of 973 K so that it can be introduced into stage A, by receiving heat from stream 8 at 995 K and from stream 28 at 1033 K, after the heat from the latter has been used to heat the rinse steam up to 973 K. At the same time, the NG-steam charge for stage C′ (stream 15) at 588 K is heated up to 763 K before it is fed into the adiabatic pre-reformer by means of the heat recovered from stream 21 at 907 K. After the pre-reformer, the gas mixture at around 714 K is expanded to 130 kPa to compensate for the pressure drop when passing through stages C′ and C, and the pressure loss associated with the heat exchangers (accounting for around 30 kPa). The pressure loss between stages C and C′ is estimated to be around 20 kPa, assuming gas velocities for these stages of around 5–6 m/s [49]. After expansion, the pre-reformed gas that has now cooled to 488 K is mixed with the PSA-off gas pre-heated to 438 K by stream 21. The resulting fuel mixture is heated up to 973 K in one step using the heat recovered from the same stream 21 at 1103 K. Intermediate pressure steam at 523 K and 1600 kPa available in the process is expanded to 600 kPa, although it has not been included in Fig. 4 for the sake of simplicity. As explained in the next section, this low pressure steam can also be exported to utilities in refineries, and therefore this exported steam figures as an efficiency credit in the performance indexes listed and explained below.

The heat recovery system depicted in Fig. 4 corresponds to the composite curves drawn in Fig. 5. These represent the main gas streams in the Ca/Cu process (CO_2-rich from stage C, H_2-rich from stage A–A0, and N_2-rich from stage B′). As can be seen in Fig. 5, the pinch point between the curves is located at the steam side of the evaporator inlet and sets the maximum steam production from the hot gas streams available in the Ca/Cu process. When evaluating the total high temperature (i.e. above the pinch point) heat available in the process (Fig. 6), it was found that nearly 70% comes from the N_2-rich gas from stage B′ and from H_2-rich gas before the PSA unit, due to their high mass flow rates and high temperatures. At the same time, the non-recycled gas from stage B (expanded in unit E) represents the lowest contribution to the total high temperature heat available. This contribution is around 3%, which means that the temperature of the non-recycled gas sent to the expander does not significantly affect the total amount of steam produced. However, expander E represents the largest power output source in the system and contributes to an important reduction of the power required by the process. The heat recovered from cooling the CO_2-rich gas stream before it is purified and compressed also represents an important source of heat in the Ca/Cu system (around 20%).

According to the operating temperatures T_{max} and T_{gin} for the different stages of the Ca/Cu looping process, and for a fixed S/C ratio of 1 in stage C′, S/C values higher than 4 are not feasible since

Table 3
Temperature, pressure, flow rate and composition of the main gas streams in Fig. 2, for operating conditions in Table 1 and S/C of 4 in stage A.

Stream	T (K)	P (kPa)	M (kmol/s)	Molar Composition (%)							
				CH_4	CO	CO_2	C_{2+}	H_2	H_2O	N_2	O_2
1	288.0	1900	0.13	89.00	0.00	2.00	8.11	0.00	0.00	0.89	0.00
2	567.0	1600	0.59	16.61	0.00	0.37	1.51	0.38	80.96	0.17	0.00
3	695.3	1564	0.62	16.82	0.03	2.51	0.00	7.38	73.11	0.16	0.00
4	973.0	1500	0.62	16.82	0.03	2.51	0.00	7.38	73.11	0.16	0.00
5	973.0	1498	0.71	1.48	1.20	0.94	0.00	57.65	38.58	0.14	0.00
6	973.0	1498	0.09	1.48	1.20	0.94	0.00	57.65	38.58	0.14	0.00
7	1143.0	1485	0.09	0.36	2.11	1.07	0.00	59.80	36.51	0.14	0.00
8	995.5	1485	0.71	1.33	1.32	0.96	0.00	57.94	38.31	0.14	0.00
9	425.3	1381	0.71	1.33	1.32	0.96	0.00	57.94	38.31	0.14	0.00
10	304.0	1365	0.37	0.00	0.00	0.00	0.00	100.00	0.00	0.00	0.00
11	400.0	2900	0.37	0.00	0.00	0.00	0.00	100.00	0.00	0.00	0.00
14	438.0	130	0.07	13.65	13.57	9.82	0.00	59.35	2.20	1.41	0.00
15	587.5	1600	0.05	42.28	0.00	0.95	3.85	0.97	51.52	0.42	0.00
16	714.3	1564	0.05	44.81	0.09	3.67	0.00	8.09	42.93	0.40	0.00
17	487.8	130	0.05	44.81	0.09	3.67	0.00	8.09	42.93	0.40	0.00
18	462.0	130	0.12	27.21	7.72	7.27	0.00	37.13	19.69	0.98	0.00
20	1143.0	122	0.18	1.34	26.44	0.28	0.00	70.39	0.90	0.65	0.00
21	1103.0	113	0.28	0.00	0.00	49.94	0.00	0.00	49.63	0.44	0.00
23	288.0	101	0.45	0.00	0.00	0.00	0.00	0.00	0.00	79.0	21.0
24	690.1	150	0.45	0.00	0.00	0.00	0.00	0.00	0.00	79.0	21.0
25	473.0	150	2.76	0.00	0.00	1.97	0.00	0.00	0.00	94.62	3.42
26	1058.5[a]	1476	2.68	0.00	0.00	2.35	0.00	0.00	0.00	97.65	0.00
27	1058.5[a]	1476	2.31	0.00	0.00	2.35	0.00	0.00	0.00	97.65	0.00
28	649.9[b]	1464	2.31	0.00	0.00	2.35	0.00	0.00	0.00	97.65	0.00
31	592.3	104	0.36	0.00	0.00	2.35	0.00	0.00	0.00	97.65	0.00

[a] Average exhaust gas temperature during stage B operation (minimum and maximum gas temperatures during this stage are 1049.0 and 1103.0 K, respectively).
[b] Average exhaust gas temperature during stage B′ operation (minimum and maximum gas temperatures during this stage are 473.0 and 1049.0 K, respectively).

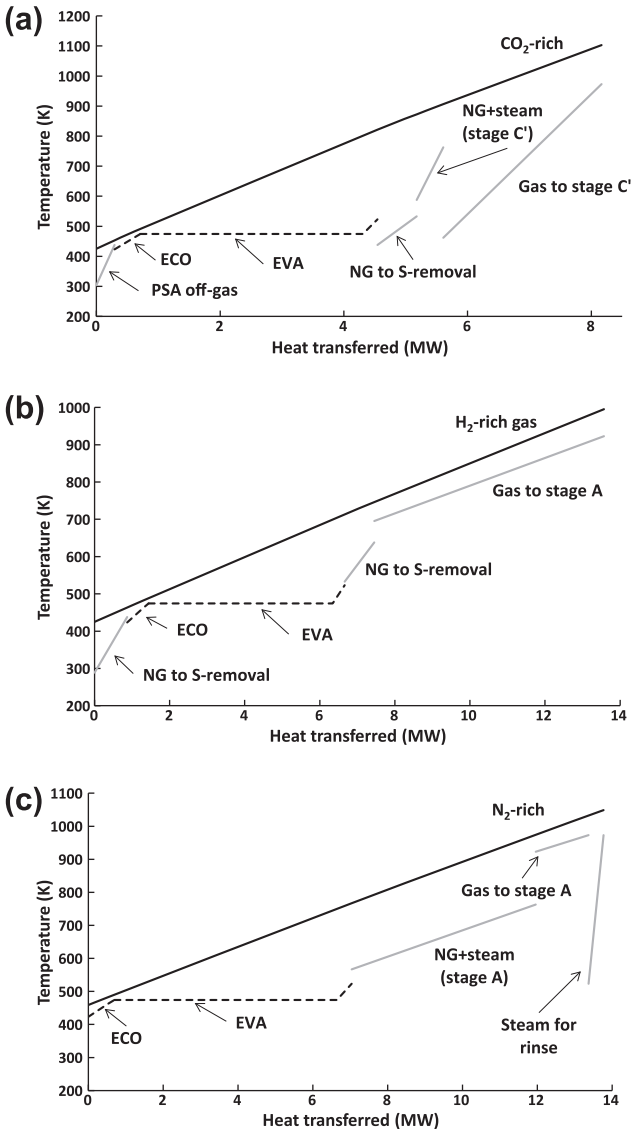

Fig. 5. Composite curves (temperature vs. heat transferred) for (a) CO_2-rich gas from stage C (stream 21); (b) H_2-rich gas from stages A and A0 (stream 8); (c) N_2-rich gas from stage B′ at $T_{max,A}$ (stream 28).

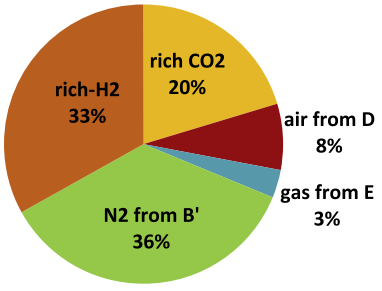

Fig. 6. Contributions to the total high temperature heat available in the Ca/Cu process from the different hot gas streams in the case at the maximum H_2 yield (S/C of 4 in stage A).

there is not enough steam available in the process at 523 K and 1600 kPa. This steam shortage imposes an upper limit for the S/C ratio in stage A and it represents a constraint since the higher the S/C ratio, the higher the H_2 yield in stage A, and therefore, the lower the NG inputs needed. However, it has been found that when working under equilibrium conditions in stage A with a S/C ratio of 4, almost 93% of the maximum H_2 yield (obtained by assuming a total conversion of the C-compounds introduced) can be achieved. Moreover, the recycling of the PSA off-gas as fuel in the reducing stage C′ of the Ca/Cu looping process prevents the emission of C-based compounds to the atmosphere. In this way the CO_2 capture rate can be maintained at a level as high as 94%.

4. Reference H_2 production plants with and without CO_2 capture

Reference H_2 production plants with and without CO_2 capture by conventional technologies are included for purposes of comparison. The reference plants are based on conventional technologies for H_2 production and utilise a fired tubular reformer (FTR) for methane conversion, as commonly installed in refineries [88–90]. A typical H_2 output of 30,000 m^3 N/h is assumed for purposes of comparison with the Ca/Cu process.

The configuration of the plant with CO_2 capture is shown in Fig. 7. After the desulphurisation step, NG is mixed with steam and sent to an adiabatic pre-reformer operating at 3200 kPa. A S/C molar ratio of 4 has been assumed, which ensures a satisfactory overall methane conversion and an appropriate steam-to-dry gas ratio at the high temperature of the WGS inlet. The pre-reformed charge is sent to the FTR, which has been designed to achieve an outlet reformed gas temperature of 1163 K. At the FTR exit, the reformed syngas is cooled down by producing saturated high pressure steam (at 10,000 kPa). This configuration avoids problems related with metal dusting, since the evaporating water keeps tubes below the critical temperature for its initiation. Syngas, once cooled to 603 K, is sent to a high temperature WGS reactor, where most of the CO is converted to CO_2, enhancing the H_2 content in the syngas. After being cooled to 473 K, the CO is further converted to CO_2 in a low temperature WGS reactor, so that at the exit about 90% of the initial carbon is present in the syngas as CO_2.

Syngas from the WGS section is then cooled to nearly ambient temperature and sent to a chemical absorption section for CO_2 separation. CO_2 capture is performed by means of a methyldiethanolamine (MDEA) chemical absorption process [91], in which about 95% of the CO_2 is selectively removed, generating a H_2-rich stream. The high-purity CO_2 released in the stripper (whose reboiler requires 0.82 MJ_{th} from the condensation of 600 kPa steam per kg of CO_2 captured) is cooled, dried and compressed to the final pressure of 11,000 kPa. The CO_2-lean H_2-rich stream from the MDEA process is then partly sent to the PSA unit for further purification, where the final H_2 product is obtained, and partly mixed with the PSA off-gases to be used as fuel in the FTR burners. By using a carbon-lean fuel in the FTR burners, it is possible to reach a carbon capture ratio of about 85%, assuming the S/C and the reactor temperatures mentioned above.

The reference FTR plant without CO_2 capture differs from the configuration described above in that there is no CO_2 absorption section, there is no low-temperature WGS reactor and for the use of NG as fuel in the FTR burners. Hence syngas at the exit of the high temperature WGS is cooled to nearly ambient temperature and sent to the PSA purification unit, where pure hydrogen is delivered and off-gases enriched with CO and CO_2 are burned in the FTR furnace after they have been mixed with additional untreated NG. The lack of a low temperature WGS reactor simplifies the operation of the plant and does not represent an energy penalty for the process, since the unconverted CO is used afterwards as fuel in the FTR. For the same reason, in the plant without CO_2 capture S/C is reduced to 2.7, which improves the overall efficiency of the process.

In both plants, enough excess heat is available from syngas and furnace flue gas cooling to guarantee the required S/C ratio in the

reformer. Thus, heat is mainly recovered by producing high pressure steam (10,000 kPa), and a backpressure steam turbine propelled by the expanding steam is used to further improve the efficiency of the overall process. Steam is first expanded to an intermediate pressure of 4000 kPa, at which point part of the steam is extracted to make up the reforming charge. The remaining steam available is further expanded to 600 kPa and is partly used for CO_2 stripping (when the CO_2 absorption unit is used) and partly exported to other units in the refinery. It should be noted that the high pressure evaporation level of 10,000 kPa is higher than that adopted in most hydrogen plants. It was selected for this study as being a good assumption for benchmark plants and to allow a fairer comparison with mid-long term plants that are equipped with advanced technology and have as their aim low emissions and high levels of efficiency.

5. Discussion

Different performance indexes were defined in order to facilitate comparison between the results obtained in the simulation of the Ca/Cu process and the reference H_2 plants with and without CO_2 capture. Defining these indexes is not straightforward, since each plant exports different amounts of steam and exchanges (both import and export) electricity with the grid. The following indexes were considered to assess the global performance of the plants:

- *H_2 production efficiency*: this is the ratio between the LHV energy output of the hydrogen stream and the LHV energy input of the natural gas fed to the plant:

$$\eta_{H_2} = \frac{\dot{m}_{H_2} \cdot LHV_{H_2}}{\dot{m}_{NG} \cdot LHV_{NG}} \tag{10}$$

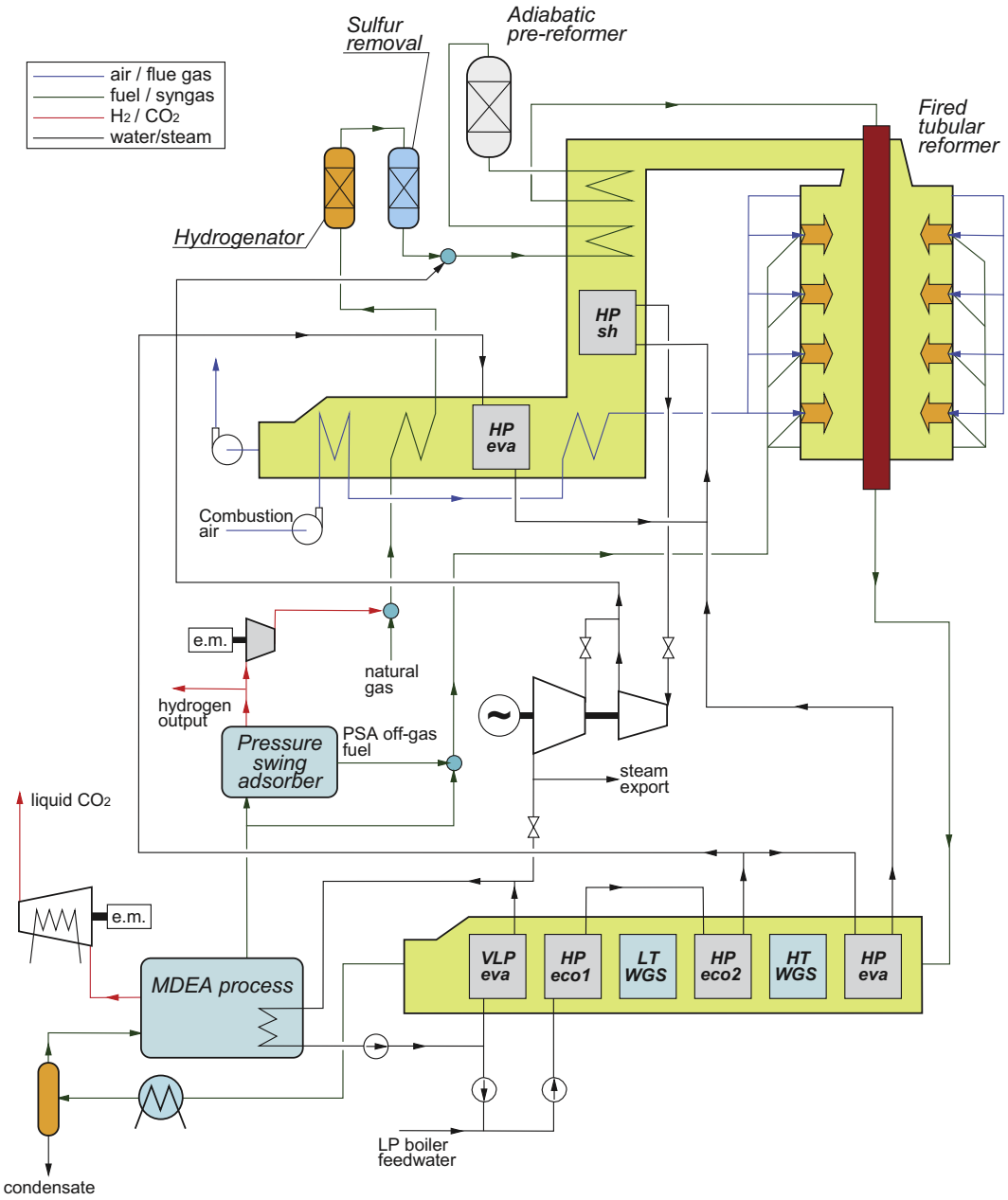

Fig. 7. Layout of the H_2 production plant with CO_2 capture included for a comparison.

where $\dot{m}_{H_2}$ is the mass flow rate of the H_2 output and $\dot{m}_{NG}$ is the mass flow rate of the natural gas input.• *Equivalent natural gas input*: this is calculated by subtracting the flow rate conceptually associated with the production of the heat Q_{th} and the electricity W_{el} exported from the plant (negative if imported) from the natural gas input:

$$\dot{m}_{NG,eq} = \dot{m}_{NG} - \frac{Q_{th}}{\eta_{th,ref} \cdot LHV_{NG}} - \frac{W_{el}}{\eta_{el,ref} \cdot LHV_{NG}} \quad (11)$$

Reference efficiencies for heat production ($\eta_{h,ref}$) and power generation ($\eta_{el,ref}$) were assumed to be 90% and 58.3% respectively, corresponding to state-of-the-art industrial boilers and large-scale combined cycles [92]. Heat export is considered proportional to the flow rate of steam exported and is calculated by assuming that steam is condensed to a saturated liquid condition.

- *Equivalent H_2 production efficiency*: this is calculated by considering the LHV power associated with the equivalent natural gas as thermal input, when natural gas is devoted to hydrogen production:

$$\eta_{eq,H_2} = \frac{\dot{m}_{H_2} \cdot LHV_{H_2}}{\dot{m}_{NG,eq} \cdot LHV_{NG}} \quad (12)$$

This index allows a homogeneous comparison to be made between the thermal performances of plants that produce different amounts of the three final products.

- *Carbon capture ratio:* this is the ratio between the CO_2 captured in the process and the CO_2 emissions related to the carbon content of the natural gas input:

$$CCR = \frac{\dot{m}_{CO_2,capt}}{\dot{m}_{NG} \cdot e_{CO_2,NG}} \quad (13)$$

where $e_{CO2,NG}$ represents the natural gas emission factor, equal to 2.65 $kgCO_2/kg_{NG}$.

- *Equivalent carbon capture ratio:* this is the ratio between the CO_2 captured in the plant and the CO_2 emissions associated with the equivalent natural gas input:

$$CCR_{eq} = \frac{\dot{m}_{CO_2,capt}}{\dot{m}_{NG,eq} \cdot e_{CO_2,NG}} \quad (14)$$

- *Equivalent CO_2 specific emissions:* this is the ratio between the CO_2 emitted, considering the CO_2 emissions related to the equivalent natural gas input, and the hydrogen output (in gCO_2 per MJ of H_2 output):

$$E_{eq} = \frac{\dot{m}_{NG,eq} \cdot e_{CO_2,NG} - \dot{m}_{CO_2,capt}}{\dot{m}_{H_2} \cdot LHV_{H_2}} \cdot 1000 \quad (15)$$

- *Equivalent specific primary energy consumption for CO_2 avoided ($SPECCA_{eq}$):* this coefficient measures the amount of fuel thermal energy required to avoid the emission of one kg of CO_2. The $SPECCA_{eq}$ (in MJ/kg CO_2) is defined as follows:

$$SPECCA_{eq} = \frac{\left(\frac{1}{\eta_{eq,H_2}} - \frac{1}{\eta_{eq,H_2-ref}}\right)}{E_{eq-ref} - E_{eq}} \cdot 1000 \quad (16)$$

where $\eta_{eq,H2\text{-}ref}$ and $E_{eq\text{-}ref}$ are the equivalent H_2 production efficiency and the equivalent specific CO_2 emissions, respectively, of the reference FTR plant without capture.

Table 4 summarises plant performance indexes obtained for the reference plants with and without CO_2 capture, together with those obtained for the Ca/Cu process under different S/C ratios in stage A according to the operating conditions detailed in Table 1. The most relevant influence of the S/C ratio in stage A lies in the NG thermal input required for the process. This increases from 112.9 MW to 117.4 MW when the S/C ratio decreases from 4 to 3, due mainly to the reduction in CH_4 conversion from 90% to 80%. At the highest S/C ratio possible in this process (i.e. 4), a η_{H2} as high as 79.1% can be achieved, which is a value far larger than the ones attained by the reference plants, either with and without CO_2 capture (69–74%). Moreover, the Cu/CaO molar ratio is slightly higher in those conditions with a S/C ratio of 3 as a consequence of two different effects. On the one hand, the lower the S/C ratio in stage A, the higher the content of CH_4 in the PSA off-gas due to the lower conversion in the SER stage. Therefore, because of the less favourable CuO reduction stoichiometry with CH_4 (reaction 9), a higher amount of Cu is required in stage C, and consequently for the process as a whole. On the other hand, when the S/C ratio decreases in stage A, the SER equilibrium is not as favoured as

Table 4
Results obtained for reference plant without/with CO_2 capture and for the Ca/Cu looping process under different operating conditions analysed, maintaining a H_2 output of 30,000 m^3 N/h in every case.

	Reference FTR based plant	Reference FTR based plant with CO_2 capture	Ca/Cu looping process[a]		Ca/Cu looping process[b]
S/C at reformer inlet (stage A for the Ca/Cu)	2.70	4	4	3	3
NG thermal input (MW)	121.94	130.79	112.87	117.39	113.56
% NG input to reformer or stage A	88.87	100.0	82.16	85.51	88.11
Steam turbine electric output (MW)	3.34	3.84	0.04	0.52	0.29
Pre-reformed gas expansion (MW)	–	–	0.49	0.41	0.33
N_2 expander (MW)	–	–	5.18	6.04	5.59
Air compressor consumption (MW)	–	–	5.84	6.53	5.95
CO_2 compressor electric consumption (MW)	–	2.15	2.12	2.21	2.13
H_2 compressor (MW)	–	–	1.07	1.06	1.06
Stage B-B′ fan (MW)	–	–	1.18	1.42	1.02
Other plant auxiliaries (MW)	0.96	1.35	0.19	0.16	0.15
Net electric plant output (MW)	2.38	0.34	−4.69	−4.41	−4.10
Heat Output (MW)	8.62	4.06	0.92	7.54	4.33
Equivalent NG thermal input (MW)	108.27	125.69	119.88	116.61	115.78
η_{H2} (%)	73.98	68.78	79.12	76.05	78.63
$\eta_{eq,H2}$ (%)	83.33	71.57	74.49	76.56	77.13
Equivalent CO_2 emission (gCO_2/MJ of H_2)	68.39	9.26	8.69	4.21	6.45
CCR (%)	–	84.92	94.15	93.71	93.05
CCR_{eq} (%)	–	88.37	88.65	94.34	91.27
Cu/CaO molar ratio	–		1.58	1.64	1.61
$SPECCA_{eq}$ (MJ/kg CO_2)	–	3.33	2.38	1.65	1.56

[a] Operating conditions described in Table 1.
[b] Modified operating conditions: 0.15 g Pt-based catalyst/g sorbent, $T_{max,B}$ = 1113 K and gas velocity of 1 m/s in stages B and B′ (the rest of operating parameters are the same as those in Table 1).

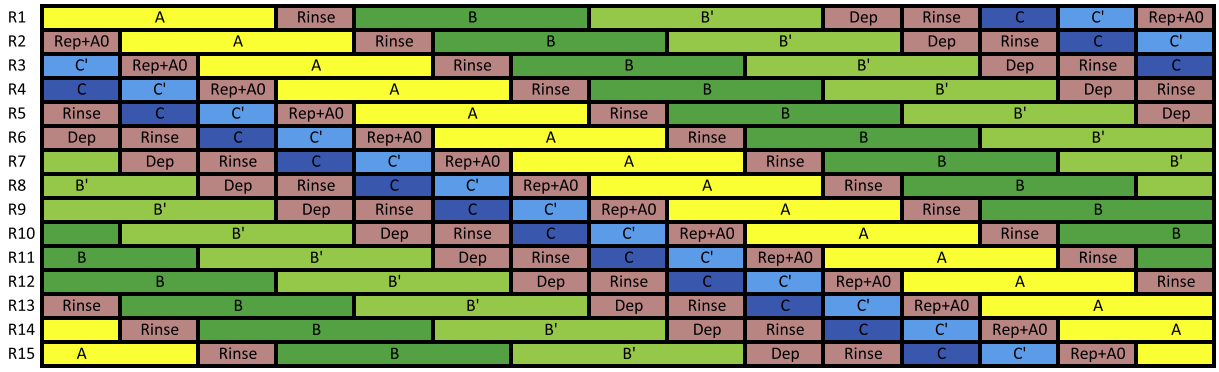

Fig. 8. Estimation of the operational diagram of the Ca/Cu looping process depicted in Fig. 2 (Notation used: dep-depressurisation; rep-pressurisation).

when the S/C ratios are high and T_{max} achieved in stage A is therefore lower, which increases the temperature difference between stages B′ and C. Consequently, the amount of energy required in stage C from the CuO reduction is greater. In contrast, $\eta_{eq,H2}$ shows the opposite behaviour by falling sharply from 76.6% to 74.5% when the S/C ratio increases from 3 to 4. This tendency is mainly due to the higher amount of steam exported for a reduced S/C ratio in stage A, caused by a lower steam requirement in stage A, and a higher level of steam production (the amount of heat available from the gas streams depicted in Fig. 4 is greater, associated with the higher recycle from B to B′, a higher fraction of gas exiting A sent to stage A0 and the higher mass flow rate of gas from stage C). The results in Table 4 show that there are no significant differences in the power output of the plant when the S/C ratio in stage A changes, because the larger steam turbine and expander outputs at reduced S/C ratios are partly compensated for by the higher consumptions of the air compressor and recycle blower.

For the reference FTR-plant with a CO_2 capture system based on MDEA absorption, a $\eta_{eq,H2}$ of around 71.6% and a carbon capture ratio (CCR) of around 85% are obtained. Noticeably better $\eta_{eq,H2}$ values for the Ca/Cu looping process result for any of the S/C ratios analysed (between 3 and 5% points above that of the reference case), mainly due to the better cold gas efficiency of the SER process. Moreover, the CCR in the Ca/Cu process is appreciably higher compared to that of the reference plant (94% vs. 85%) since carbon emissions associated with the PSA off-gas are avoided. These differences translate into a lower amount of energy consumed per unit of CO_2 captured in the Ca/Cu process (i.e. around 1.6–2.4 MJ/kg of CO_2) compared to that of the reference plant with capture (3.3 MJ/kg of CO_2), which confirms the potential of this novel Ca/Cu process as a good H_2 production technology with CO_2 capture compared to conventional H_2 production processes equipped with commercial capture technologies.

As can be seen from results in Table 4, the main power consumptions correspond to the air compressor that supplies O_2 in the oxidation stage of the Ca/Cu process. The operating conditions selected in this work (detailed in Table 1) offer several alternatives for improving the performance of the process while lowering the power requirements. The use of more reactive reforming catalysts based on noble transition metals (such as Pt, Rh or Pt), that do not undergo oxidation and reduction over the several reaction stages, reduces the amount of catalyst needed in the process and reduces air consumption in the oxidation stage. Other alternatives that would improve the performance of the Ca/Cu looping process include increasing the maximum temperature allowed in stage B, which would reduce the amount of Cu-material and solid material to be heated up in stage C. Also reducing the gas velocities in stages B and B′ would result in lower pressure drop in the solid bed and, therefore, in a lower consumption of the recycle blower. In order to quantify the influence of these alternatives on the performance of the process, an additional simulation case based on the following assumptions has been included: (1) a Pt-based reforming catalyst, working under the minimum catalyst-to-sorbent mass ratio of 0.15 required to achieve the maximum possible H_2 production [51], (2) a maximum temperature in stage B of 1113 K, and (3) a gas velocity in stages B and B′ of 1 m/s. The results obtained under these conditions have been listed in the last column of Table 4. As expected, a reduction in the power needed in the process is observed because of the smaller amount of air consumed in the oxidation stage resulting from the use of a noble metal catalyst, and from the reduction in the pressure drop in the recycle blower. Moreover, the η_{H2} and $\eta_{eq,H2}$ values increase to 78.6% and 77.1%, respectively, with respect to the Ca/Cu base case with a S/C ratio of 3 under the conditions in Table 1, due to the reduced energy input needed in stage C′ associated with the smaller amount of solid material required and the lower temperature difference to be heated up to reach the calcination temperature during stage C. These results show there is potential for efficiency improvement in the Ca/Cu looping process if more active catalysts are used, and if higher maximum temperatures or lower gas velocities are allowed during the reaction stages. In addition to the alternatives already analysed, the development of materials with a higher content of active CaO or Cu than those considered in this work could also contribute to a reduction in the energy consumption of the Ca/Cu process, and therefore to an enhancement of its performance. For this reason, further investigation focused on materials for the Ca/Cu process with low inert and high active contents is needed to confirm the experimental and modelling potential of this novel concept.

In a continuous process, all the reaction stages described above must be carried out in a system of packed fixed beds operating in a cyclical manner. Multiple beds operating at the same time with the feed gas being switched from one reactor to another reactor are necessary to produce the steady amount of H_2 mentioned above (30,000 Nm^3/h). For the operating conditions and flow rates that maximise H_2 efficiency (a S/C of 4 in stage A), and a reactor length of 7 m, a theoretical duration of around 30 min has been estimated for stage A assuming that the essential design criterion for this stage is to work at the highest possible gas velocity (0.5 m/s) allowed by the SER equilibrium [50]. For stages B and B′, the criterion followed has been the minimum number of beds working in parallel without incurring an unacceptably high pressure loss. An acceptable limit for the pressure drop in a reaction stage is considered to be around 50 kPa. Therefore, gas velocities of around 2 m/s (B) and 1 m/s (B′) have been chosen. In stages C and C′, the reduction, calcination and reforming reactions are fast enough to permit the operation at a high gas velocity (around 5–6 m/s) without incurring an excessive pressure loss. A theoretical time for the completion of one cycle has been estimated to be around

140 min assuming a minimum of 15 reactors: 3 operating in stage A, 3 in stage B, 3 in stage B′, and one reactor for each of the other remaining steps (stage C, stage C′, rinse steps (2), depressurisation and re-pressurisation + stage A0), as shown in Fig. 8. The operational diagram proposed in this work is based on simple process assumptions, and therefore, an alternative diagram would be possible if a more complete economic assessment were carried out so as to optimize the process in terms of velocities, number of parallel reactors, reactor length, etc.

A further point to be discussed is the temperature of the gas from B stage which is expanded in the N_2 expander. In order to avoid thermal stress affecting the turbine blades and pressure fluctuations, temperature variations and gradients need to be minimised. It is generally acknowledged that the smaller the temperature change of the gas sent to the N_2 expander, the better for turbine operation. Similarly, mixing the outlet gas from the beds operating in parallel in stage B with a certain time shifting could have a positive buffering effect, leading to smoother temperature peaks. In the case of S/C = 4, the maximum ΔT of 54 K for the gas from stage B (between $T_{max,A}$ = 1049 K and $T_{max,B}$ = 1103 K) is reduced to 18 K as a result of operating with three parallel beds.

As a final remark, it should be highlighted that an economic analysis is needed to evaluate the feasibility of this concept compared to competitive technologies. The controllability of the plant, the availability and reliability are other important points to be taken into account when comparing different processes. As regards capital cost, despite a number of parallel reactors are required in the Ca/Cu process, cheaper material than in FTR can be used and downstream shift reactors and equipment for CO_2 separation are avoided, with potential savings. As far as operating costs are concerned, the high hydrogen production efficiencies obtained with the Ca/Cu process can be decisive, considering that operating cost in conventional FTR plants, associated to primary feedstock consumption, can contribute by up to 70–85% to the cost of the hydrogen produced [93].

6. Conclusions

A detailed and complete process design of a H_2 production plant based on a novel Ca/Cu chemical looping process has been described assuming a set of reasonable operating conditions (0.3 g of conventional Ni-based catalyst per g of CO_2 sorbent, 1600 kPa, a maximum temperature in the oxidation stage of around 1103 K and a maximum temperature for the sorbent calcination of around 1143 K). On the basis of a fully integrated scheme representing the gas streams available in the Ca/Cu process and a complete thermodynamic assessment, this study estimates a maximum H_2 yield of 3.4 mol of H_2/mol of carbon, which corresponds to an equivalent hydrogen efficiency of around 75% and a CCR of around 94%. Following an analogous procedure for the integration of a reference H_2 production plant based on conventional steam reforming with MDEA for CO_2 absorption, an equivalent hydrogen efficiency of around 72% (3% points lower than the Ca/Cu process) was obtained with a CCR of around 85% (9% points lower).

It has been demonstrated that the use of more reactive reforming catalysts (based on noble transition metals), higher temperatures during Cu oxidation and lower gas velocities to reduce the pressure drop, improve the equivalent hydrogen efficiency of the Ca/Cu looping process by as much as 77%. Under these conditions, the equivalent specific energy consumption in the Ca/Cu looping plant is 1.6 MJ/kg of CO_2 captured with a CCR of 93%, which is much lower than the energy consumed in the reference plant with CO_2 capture (3.3 MJ/kg CO_2 captured) with a lower CCR. These results, added to other design advantages inherent in a Ca/Cu looping process with a compact pressurised reactor design, demonstrate the potential of this novel process as a H_2 production technology with CO_2 capture compared to conventional H_2 production processes that use commercial capture technologies. Further research on materials with a higher content of active CaO or Cu to minimize the inert content of solid beds will also contribute to reducing energy consumption in this process and to a better plant performance.

Acknowledgements

This work is supported by the R+D Spanish National Program from the Spanish Ministry of Economy and Competitiveness under Project ENE2012-37936-C02-01 and from CSIC 201280E017. Financial support for the PhD of I. Martínez is provided by the FPU programme of the Spanish Ministry of Education (AP2009-3575), and funding to carry out this work has been provided by the Europe programme of the CAI.

References

[1] Meerman JC, Hamborg ES, van Keulen T, Ramírez A, Turkenburg WC, Faaij APC. Techno-economic assessment of CO_2 capture at steam methane reforming facilities using commercially available technology. Int J Greenhouse Gas Control 2012;9:160–71.
[2] Simbeck DR. CO_2 capture and storage–the essential bridge to the hydrogen economy. Energy 2004;29(9–10):1633–41.
[3] Weydahl T, Jamaluddin J, Seljeskog M, Anantharaman R. Pursuing the pre-combustion CCS route in oil refineries – The impact on fired heaters. Appl Energy 2013;102:833–9.
[4] Romano MC, Anantharaman R, Arasto A, Ozcan DC, Ahn H, Dijkstra JW, et al. Application of advanced technologies for CO_2 capture from industrial sources. Energy Procedia 2013;37:7176–85.
[5] Bockris JOM. The origin of ideas on a hydrogen economy and its solution to the decay of the environment. Int J Hydrogen Energy 2002;27(7–8):731–40.
[6] Metz B, Davidson O, de Coninck H, Loos M, Meyer L. IPCC special report on carbon dioxide capture and storage. Prepared by Working Group III of the Intergovernmental Panel on Climate Change. Cambridge (NY, USA): Cambridge University Press; 2005: p. 442.
[7] IEA. Energy Technology Analysis. CO_2 capture and storage – A key carbon abatement option. 2008.
[8] Rostrup-Nielsen JR, Sehested J, Nørskov JK. Hydrogen and synthesis gas by steam- and CO_2 reforming. Adv Catal: Academic Press; 2002: p. 65–139.
[9] Rostrup-Nielsen T. Manufacture of hydrogen. Catal Today 2005;106(1–4):293–6.
[10] Olsson H, Rudbeck P, Andersen KH. Adding hydrogen production capacity by heat exchange reforming XIV refinery technology meet (RTM). Kovalam (Trivandrum, India): Energy & Environment Challenges for the Hydrocarbon Sector; 2007.
[11] Klett MG, White JS, Schoff RL, Buchanan TL. Hydrogen production facilities plant performance and cost comparisons. US Department of Energy (DOE)/ National Energy Technology Laboratory (NETL): Final Report; 2002.
[12] Rostrup-Nielsen JR. Steam reforming and chemical recuperation. Catal Today 2009;145(1–2):72–5.
[13] Young DJ, Zhang J, Geers C, Schütze M. Recent advances in understanding metal dusting: a review. Mater Corros 2011;62(1):7–28.
[14] Grabke HJ. Corrosion by carbonaceous gases, carburization and metal dusting, and methods of prevention. Mater High Temp 2000;17(4):483–7.
[15] Balasubramanian B, Lopez Ortiz A, Kaytakoglu S, Harrison DP. Hydrogen from methane in a single-step process. Chem Eng Sci 1999;54(15–16):3543–52.
[16] Johnsen K, Ryu HJ, Grace JR, Lim CJ. Sorption-enhanced steam reforming of methane in a fluidised bed reactor with dolomite as -acceptor. Chem Eng Sci 2006;61(4):1195–202.
[17] Adris AM, Elnashaie SSEH, Hughes R. A fluidised bed membrane reactor for the steam reforming of methane. Can J Chem Eng 1991;69(5):1061–70.
[18] Chen Z, Prasad P, Yan Y, Elnashaie S. Simulation for steam reforming of natural gas with oxygen input in a novel membrane reformer. Fuel Process Technol 2003;83(1–3):235–52.
[19] Chen Z, Po F, Grace JR, Jim Lim C, Elnashaie S, Mahecha-Botero A, et al. Sorbent-enhanced/membrane-assisted steam-methane reforming. Chem Eng Sci 2008;63(1):170–82.
[20] Chen Z, Yan Y, Elnashaie SSEH. Novel circulating fast fluidised-bed membrane reformer for efficient production of hydrogen from steam reforming of methane. Chem Eng Sci 2003;58(19):4335–49.
[21] Jordal K, Bredesen R, Kvamsdal HM, Bolland O. Integration of H_2-separating membrane technology in gas turbine processes for CO_2 capture. Energy 2004;29(9–10):1269–78.
[22] Fayyaz B, Harale A, Park B-G, Liu PKT, Sahimi M, Tsotsis TT. Design Aspects of hybrid adsorbent−membrane reactors for hydrogen production. Ind Eng Chem Res 2005;44(25):9398–408.

[23] Jansen D, Dijkstra JW, van den Brink RW, Peters TA, Stange M, Bredesen R, et al. Hydrogen membrane reactors for CO_2 capture. Energy Procedia 2009;1(1):253–60.
[24] Chiesa P, Romano MC, Kreutz TG. Use of membranes in systems for electric energy and hydrogen production from fossil fuels. In: Basile A, editor. Handbook of membrane reactors: Woodhead Publishing Limited; 2013.
[25] Chiesa P, Romano MC, Spallina V, Turi DM, Mancuso L. Efficient low CO_2 emissions power generation by mixed conducting membranes. Energy Procedia 2013;37:905–13.
[26] Han C, Harrison DP. Simultaneous shift reaction and carbon dioxide separation for the direct production of hydrogen. Chem Eng Sci 1994;49(24, Part 2):5875–83.
[27] Hufton JR, Mayorga S, Sircar S. Sorption-enhanced reaction process for hydrogen production. AIChE J 1999;45(2):248–56.
[28] Johnsen K, Grace JR, Elnashaie SSEH, Kolbeinsen L, Eriksen D. Modeling of sorption-enhanced steam reforming in a dual fluidised bubbling bed reactor. Ind Eng Chem Res 2006;45(12):4133–44.
[29] Yi KB, Harrison DP. Low-pressure sorption-enhanced hydrogen production. Ind Eng Chem Res 2005;44(6):1665–9.
[30] Brun-Tsekhovoi AR, Zadorin AN, Katsobashvili YR, Kourdyumov SS. The process of catalytic steam reforming of hydrocarbons in the presence of carbon dioxide acceptor. In: Press P, editor. Hydrocarbon energy progress VII. Moscow; 1988: p. 885.
[31] Ding Y, Alpay E. Adsorption-enhanced steam–methane reforming. Chem Eng Sci 2000;55(18):3929–40.
[32] Lopez Ortiz A, Harrison DP. Hydrogen production using sorption-enhanced reaction. Ind Eng Chem Res 2001;40(23):5102–9.
[33] Ochoa-Fernández E, Rusten HK, Jakobsen HA, Rønning M, Holmen A, Chen D. Sorption enhanced hydrogen production by steam methane reforming using Li_2ZrO_3 as sorbent: Sorption kinetics and reactor simulation. Catal Today 2005;106(1–4):41–6.
[34] G-h Xiu, Li P, Rodrigues EA. Sorption-enhanced reaction process with reactive regeneration. Chem Eng Sci 2002;57(18):3893–908.
[35] Waldron WE, Hufton JR, Sircar S. Production of hydrogen by cyclic sorption enhanced reaction process. AIChE J 2001;47(6):1477–9.
[36] Harrison DP. Sorption-enhanced hydrogen production: a review. Ind Eng Chem Res 2008;47(17):6486–501.
[37] Chen Z, Grace JR, Lim CJ. CO_2 capture and hydrogen production in an integrated fluidised bed reformer-regenerator system. Ind Eng Chem Res 2011;50(8):4716–21.
[38] Romano MC, Cassotti EN, Chiesa P, Meyer J, Mastin J. Application of the sorption enhanced-steam reforming process in combined cycle-based power plants. Energy Procedia 2011;4:1125–32.
[39] Ochoa-Fernandez E, Haugen G, Zhao T, Ronning M, Aartun I, Borresen B, et al. Process design simulation of H_2 production by sorption enhanced steam methane reforming: evaluation of potential CO_2 acceptors. Green Chem 2007;9(6):654–62.
[40] Z-s Li, N-s Cai. Modeling of multiple cycles for sorption-enhanced steam methane reforming and sorbent regeneration in fixed bed reactor. Energy Fuels 2007;21(5):2909–18.
[41] Meyer J, Mastin J, Bjørnebøle T-K, Ryberg T, Eldrup N. Techno-economical study of the zero emission gas power concept. Energy Procedia 2011;4:1949–56.
[42] Weimer T, Berger R, Hawthorne C, Abanades JC. Lime enhanced gasification of solid fuels: Examination of a process for simultaneous hydrogen production and CO_2 capture. Fuel 2008;87(8–9):1678–86.
[43] Lyon RK. Method and apparatus for unmixed combustion as an alternative to fire, 1996, Patent Number 5, 509, 362.
[44] Kumar RV, Cole JA, Lyon RK. Unmixed reforming: an advanced steam reforming process. 218th ACS National Meeting. New Orleans, LA: American Chemical Society, Division of Fuel, Chemistry; 1999. p. 894–8.
[45] Kumar RV, Lyon RK, Cole JA. Unmixed reforming: a novel autothermal cyclic steam reforming process. In: Gregoire Padro CEaL, F., editor. Adv Hydrogen Energy. New York, Boston, Dordrecht, London, Moscow: Kluwer Academic Publishers; 2002: p. 31–46.
[46] Dupont V, Ross AB, Knight E, Hanley I, Twigg MV. Production of hydrogen by unmixed steam reforming of methane. Chem Eng Sci 2008;63(11):2966–79.
[47] Abanades JC, Murillo R. Method for recovering CO_2 by means of CaO and the exothermic reduction of a solid. WO/2011/033156, September 2009.
[48] Feng B. Sorbent regeneration. WO 2011/082448 A1, January 2010.
[49] Fernández JR, Abanades JC, Murillo R, Grasa G. Conceptual design of a hydrogen production process from natural gas with CO_2 capture using a Ca–Cu chemical loop. Int J Greenhouse Gas Control 2012;6:126–41.
[50] Fernández JR, Abanades JC, Murillo R. Modeling of sorption enhanced steam methane reforming in an adiabatic fixed bed reactor. Chem Eng Sci 2012;84:1–11.
[51] Fernández JR, Abanades JC, Grasa G. Modeling of sorption enhanced steam methane reforming–Part II: Simulation within a novel Ca/Cu chemical loop process for hydrogen production. Chem Eng Sci 2012;84:12–20.
[52] Qin C, Yin J, Liu W, An H, Feng B. Behavior of CaO/CuO based composite in a combined calcium and copper chemical looping process. Ind Eng Chem Res 2012;51(38):12274–81.
[53] Manovic V, Anthony EJ. Integration of calcium and chemical looping combustion using composite CaO/CuO-based materials. Environ Sci Technol 2011;45(24):10750–6.
[54] Manovic V, Anthony EJ. CaO-based pellets with oxygen carriers and catalysts. Energy Fuels 2011;25(10):4846–53.
[55] Manovic V, Wu Y, He I, Anthony EJ. Core-in-Shell CaO/CuO-Based Composite for CO_2 capture. Ind Eng Chem Res 2011;50(22):12384–91.
[56] Kierzkowska AM, Muller CR. Development of calcium-based, copper-functionalised CO_2 sorbents to integrate chemical looping combustion into calcium looping. Energy Environ Sci 2012;5(3):6061–5.
[57] Martínez I, Murillo R, Grasa G, Fernández JR, Abanades JC. Integrated combined cycle from natural gas with CO_2 capture using a Ca–Cu chemical loop. AIChE J 2013;59(8):2780–94.
[58] Noorman S, Van Sint Annaland M, Kuipers. Packed bed reactor technology for chemical-looping combustion. Ind Eng Chem Res 2007;46(12):4212–20.
[59] Hamers HP, Gallucci F, Cobden PD, Kimball E, Van Sint Annaland M. A novel reactor configuration for packed bed chemical-looping combustion of syngas. Int J Greenhouse Gas Control 2013;16:1–12.
[60] Spallina V, Gallucci F, Romano MC, Chiesa P, Lozza G, Van Sint Annaland M. Investigation of heat management for CLC of syngas in packed bed reactors. Chem Eng J 2013;225:174–91.
[61] Noorman S, Van Sint Annaland M, Kuipers JAM. Experimental validation of packed bed chemical-looping combustion. Chem Eng Sci 2010;65(1):92–7.
[62] Noorman S, Gallucci F, Van Sint Annaland M, Kuipers HJAM. Experimental investigation of a CuO/Al_2O_3 oxygen carrier for chemical-looping combustion. Ind Eng Chem Res 2010;49(20):9720–8.
[63] Noorman S, Gallucci F, Van Sint Annaland M, Kuipers JAM. Experimental investigation of chemical-looping combustion in packed beds: a parametric study. Ind Eng Chem Res 2011;50(4):1968–80.
[64] Noorman S, Gallucci F, Van Sint Annaland M, Kuipers JAM. A theoretical investigation of CLC in packed beds. Part 1: particle model. Chem Eng J 2011;167(1):297–307.
[65] KOPECS. http://www.kopecs.com/products/04_desuperheater_high_temperature_valves.htm. [accessed on September 2013].
[66] Kohl AL, Nielsen RB. Gas Purification, fifth edition. Gulf Publishing Company; 1997.
[67] Fluor Daniel Inc. Electricity production and CO_2 capture via partial oxidation of natural gas. IEA, Report No. PH3/21; 2000.
[68] Rostrup-Nielsen JR. Production of synthesis gas. Catal Today 1993;18(4):305–24.
[69] Christensen TS. Adiabatic prereforming of hydrocarbons – an important step in syngas production. Appl Catal A: Gen 1996;138(2):285–309.
[70] Hughes RW, Lu D, Anthony EJ, Wu Y. Improved long-term conversion of limestone-derived sorbents for in situ capture of CO_2 in a fluidised bed combustor. Ind Eng Chem Res 2004;43(18):5529–39.
[71] Manovic V, Anthony EJ. Steam reactivation of spent cao-based sorbent for multiple CO_2 capture cycles. Environ Sci Technol 2007;41(4):1420–5.
[72] Martínez I, Grasa G, Murillo R, Arias B, Abanades JC. Evaluation of CO_2 carrying cof reactivated CaO by hydration. Energy Fuels 2011;25(3):1294–301.
[73] Anthony EJ, Bulewicz EM, Jia L. Reactivation of limestone sorbents in FBC for SO_2 capture. Progress Energy Combust Sci 2007;33(2):171–210.
[74] Lin S, Harada M, Suzuki Y, Hatano H. CaO hydration rate at high temperature (~1023 K). Energy Fuels 2006;20(3):903–8.
[75] Wang W, Ramkumar S, Wong D, Fan L-S. Simulations and process analysis of the carbonation–calcination reaction process with intermediate hydration. Fuel 2012;92(1):94–106.
[76] Curran GP, Fink CE, Gorin E. CO_2 acceptor gasification process. Fuel Gasification: American Chemical Society; 1967. p. 141–65.
[77] Paterson N, Elphick S, Dugwell DR, Kandiyoti R. Calcium-based liquid phase formation in pressurised gasifier environments. Energy Fuels 2001;15(4):894–902.
[78] Fuerstenau MC, Shen CM, Palmer BR. Liquidus temperatures in the calcium carbonate–calcium hydroxide–calcium oxide and calcium carbonate–calcium sulfate–calcium sulfide ternary systems. Ind Eng Chem Process Des Develop 1981;20(3):441–3.
[79] Lin S-Y, Suzuki Y, Hatano H, Harada M. Hydrogen production from hydrocarbon by integration of water−carbon reaction and carbon dioxide removal (HyPr−RING method). Energy Fuels 2001;15(2):339–43.
[80] Lin S, Harada M, Suzuki Y, Hatano H. Process analysis for hydrogen production by reaction integrated novel gasification (HyPr-RING). Energy Convers Manage 2005;46(6):869–80.
[81] Martínez I, Grasa G, Murillo R, Arias B, Abanades JC. Evaluation of CO_2 carrying capacity of reactivated cao by hydration. Energy Fuels 2011;25(3):1294–301.
[82] Samms JAC, Evans BE. Thermal dissociation of $Ca(OH)_2$ at elevated pressures. J Appl Chem 1968;18(1):5–8.
[83] Barker R. The reversibility of the reaction $CaCO_3 \rightleftarrows CaO + CO_2$. J Appl Chem Biotechnol 1973;23(10):733–42.
[84] Chuang SY, Dennis JS, Hayhurst AN, Scott SA. Development and performance of Cu-based oxygen carriers for chemical-looping combustion. Combust Flame 2008;154(1–2):109–21.
[85] Tagliabue M, Farrusseng D, Valencia S, Aguado S, Ravon U, Rizzo C, et al. Natural gas treating by selective adsorption: Material science and chemical engineering interplay. Chem Eng J 2009;155(3):553–66.
[86] Stöcker J, Whysale M, Miller GQ. 30 years of PSA technology for hydrogen production. http://www.uop.com/objects/30yrsPSATechHydPurif.pdf.
[87] Sircar S, Golden TC. Purification of hydrogen by pressure swing adsorption. Sep Sci Technol 2000;35(5):667–87.

[88] Aasberg-Petersen K, Bak Hansen JH, Christensen TS, Dybkjaer I, Christensen PS, Stub Nielsen C, et al. Technologies for large-scale gas conversion. Appl Catal A: General 2001;221(1–2):379–87.
[89] Dybkjaer I, Rostrup-Nielsen JR, Aasberg-Petersen K. Hydrogen and synthesis gas. Encyclopedia of Hydrocarbons. Rome: Treccani; 2007: p. 469–500.
[90] Chiesa P. Advanced technologies for syngas and hydrogen (H_2) production from fossil fuel feedstocks in power plants. In: Roddy D, editor. Adv Power Plant Mater, des Technol. Cambridge (United Kingdom): Woodhead Publishing Limited; 2010. p. 383–410.
[91] Romano MC, Chiesa P, Lozza G. Pre-combustion CO_2 capture from natural gas power plants, with ATR and MDEA processes. Int J Greenhouse Gas Control 2010;4(5):785–97.
[92] Franco F, Anantharaman R, Bolland O, Booth N, van Dorst E, Ekstrom C, et al. European best practice guidelines for assesment of CO_2 capture technologies. 2011.
[93] Bressan L, Davis C. Driving down costs in hydrogen production. Processing Shale Feedstocks. 2013: p. 23–7.